Transform Learning MRI with Global Wavelet Regularization

A. Korhan Tanc[1] Ender M. Eksioglu[2]

[1]Department of EEE
Kirklareli University
Kirklareli, Turkey

[2]Department of ECE
Istanbul Technical University
Istanbul, Turkey

EUSIPCO 2015

Outline

1. Introduction
   - The Problem
   - The Novel Approach
2. Transform Learning MRI
3. GTLMRI
   - New Cost
   - GTLMRI: Denoising
   - GTLMRI: Reconstruction
   - GTLMRI: Overall Algorithm
4. Simulations and Conclusion

Outline

1. Introduction
   - The Problem
   - The Novel Approach
2. Transform Learning MRI
3. GTLMRI
   - New Cost
   - GTLMRI: Denoising
   - GTLMRI: Reconstruction
   - GTLMRI: Overall Algorithm
4. Simulations and Conclusion

Sparse MRI

- Active research area: Use sparsity as a regularizer for ill-conditioned inverse problems.
- Sparse regularization (and compressed sensing (CS)) have been applied to image reconstruction in Magnetic Resonance Imaging (MRI) (our problem of interest).
- Pioneering work [Lustig et.al., 2007], Sparse MRI: sparsely regularize the MRI reconstruction problem.

$$\min_{x} \frac{1}{2}\|\mathcal{F}_u x - y\|_2^2 + \rho_1\|\Phi x\|_1 + \rho_2\|x\|_{TV}. \quad (1)$$

Sparse MRI

- Active research area: Use sparsity as a regularizer for ill-conditioned inverse problems.
- Sparse regularization (and compressed sensing (CS)) have been applied to image reconstruction in Magnetic Resonance Imaging (MRI) (our problem of interest).
- Pioneering work [Lustig et.al., 2007], Sparse MRI: sparsely regularize the MRI reconstruction problem.

$$\min_{x} \frac{1}{2}\|\mathcal{F}_u x - y\|_2^2 + \rho_1\|\Phi x\|_1 + \rho_2\|x\|_{TV}. \quad (1)$$

Sparse MRI

- Active research area: Use sparsity as a regularizer for ill-conditioned inverse problems.
- Sparse regularization (and compressed sensing (CS)) have been applied to image reconstruction in Magnetic Resonance Imaging (MRI) (our problem of interest).
- Pioneering work [Lustig et.al., 2007], Sparse MRI: sparsely regularize the MRI reconstruction problem.

$$\min_{\boldsymbol{x}} \frac{1}{2}\|\mathcal{F}_u \boldsymbol{x} - \boldsymbol{y}\|_2^2 + \rho_1 \|\boldsymbol{\Phi x}\|_1 + \rho_2 \|\boldsymbol{x}\|_{\mathrm{TV}}. \quad (1)$$

Sparse MRI

- Active research area: Use sparsity as a regularizer for ill-conditioned inverse problems.
- Sparse regularization (and compressed sensing (CS)) have been applied to image reconstruction in Magnetic Resonance Imaging (MRI) (our problem of interest).
- Pioneering work [Lustig et.al., 2007], Sparse MRI: sparsely regularize the MRI reconstruction problem.

$$\min_{\boldsymbol{x}} \frac{1}{2}\|\mathcal{F}_u \boldsymbol{x} - \boldsymbol{y}\|_2^2 + \rho_1 \|\boldsymbol{\Phi x}\|_1 + \rho_2 \|\boldsymbol{x}\|_{\mathrm{TV}}. \tag{1}$$

Sparse MRI

- Active research area: Use sparsity as a regularizer for ill-conditioned inverse problems.
- Sparse regularization (and compressed sensing (CS)) have been applied to image reconstruction in Magnetic Resonance Imaging (MRI) (our problem of interest).
- Pioneering work [Lustig et.al., 2007], Sparse MRI: sparsely regularize the MRI reconstruction problem.

$$\min_{\boldsymbol{x}} \frac{1}{2}\|\mathcal{F}_u \boldsymbol{x} - \boldsymbol{y}\|_2^2 + \rho_1 \|\boldsymbol{\Phi x}\|_1 + \rho_2 \|\boldsymbol{x}\|_{\mathrm{TV}}. \tag{1}$$

Sparse MRI

$$\min_{\boldsymbol{x}} \frac{1}{2}\|\mathcal{F}_u \boldsymbol{x} - \boldsymbol{y}\|_2^2 + \rho_1 \|\boldsymbol{\Phi x}\|_1 + \rho_2 \|\boldsymbol{x}\|_{\mathrm{TV}}.$$

- $\boldsymbol{x} \in \mathbb{C}^N$ is the reconstructed MR image in vectorized form.
- $\mathcal{F}_u$ is the undersampled Fourier transform operator: conversion from the vectorized image to the k-space.
- $\boldsymbol{y} = \mathcal{F}_u \boldsymbol{x}^\star + \eta \in \mathbb{C}^\kappa$ is the observation vector in the k-space.
- $\boldsymbol{x}^\star$ is the true underlying image and η is the additive noise.
- The ratio κ/N quantifies the undersampling.
- $\|\cdot\|_1$ denotes the ℓ_1 norm.
- $\boldsymbol{\Phi}$ is a sparsifying operator: we will assume it to be a square wavelet transform.
- $\|\cdot\|_{\mathrm{TV}}$ is the Total Variation (TV) norm.

Sparse MRI

$$\min_{\boldsymbol{x}} \frac{1}{2}\|\mathcal{F}_u\boldsymbol{x} - \boldsymbol{y}\|_2^2 + \rho_1\|\boldsymbol{\Phi}\boldsymbol{x}\|_1 + \rho_2\|\boldsymbol{x}\|_{\mathrm{TV}}.$$

- $\boldsymbol{x} \in \mathbb{C}^N$ is the reconstructed MR image in vectorized form.
- $\mathcal{F}_u$ is the undersampled Fourier transform operator: conversion from the vectorized image to the k-space.
- $\boldsymbol{y} = \mathcal{F}_u\boldsymbol{x}^\star + \boldsymbol{\eta} \in \mathbb{C}^\kappa$ is the observation vector in the k-space.
- $\boldsymbol{x}^\star$ is the true underlying image and $\boldsymbol{\eta}$ is the additive noise.
- The ratio κ/N quantifies the undersampling.
- $\|\cdot\|_1$ denotes the ℓ_1 norm.
- $\boldsymbol{\Phi}$ is a sparsifying operator: we will assume it to be a square wavelet transform.
- $\|\cdot\|_{\mathrm{TV}}$ is the Total Variation (TV) norm.

Sparse MRI

$$\min_{\boldsymbol{x}} \frac{1}{2}\|\mathcal{F}_u\boldsymbol{x} - \boldsymbol{y}\|_2^2 + \rho_1\|\boldsymbol{\Phi}\boldsymbol{x}\|_1 + \rho_2\|\boldsymbol{x}\|_{\mathrm{TV}}.$$

- $\boldsymbol{x} \in \mathbb{C}^N$ is the reconstructed MR image in vectorized form.
- $\mathcal{F}_u$ is the undersampled Fourier transform operator: conversion from the vectorized image to the k-space.
- $\boldsymbol{y} = \mathcal{F}_u\boldsymbol{x}^\star + \boldsymbol{\eta} \in \mathbb{C}^\kappa$ is the observation vector in the k-space.
- $\boldsymbol{x}^\star$ is the true underlying image and η is the additive noise.
- The ratio κ/N quantifies the undersampling.
- $\|\cdot\|_1$ denotes the ℓ_1 norm.
- $\boldsymbol{\Phi}$ is a sparsifying operator: we will assume it to be a square wavelet transform.
- $\|\cdot\|_{\mathrm{TV}}$ is the Total Variation (TV) norm.

Sparse MRI

$$\min_{\boldsymbol{x}} \frac{1}{2}\|\mathcal{F}_u\boldsymbol{x} - \boldsymbol{y}\|_2^2 + \rho_1\|\boldsymbol{\Phi x}\|_1 + \rho_2\|\boldsymbol{x}\|_{\mathrm{TV}}.$$

- $\boldsymbol{x} \in \mathbb{C}^N$ is the reconstructed MR image in vectorized form.
- $\mathcal{F}_u$ is the undersampled Fourier transform operator: conversion from the vectorized image to the k-space.
- $\boldsymbol{y} = \mathcal{F}_u\boldsymbol{x}^\star + \boldsymbol{\eta} \in \mathbb{C}^\kappa$ is the observation vector in the k-space.
- $\boldsymbol{x}^\star$ is the true underlying image and η is the additive noise.
- The ratio κ/N quantifies the undersampling.
- $\|\cdot\|_1$ denotes the ℓ_1 norm.
- $\boldsymbol{\Phi}$ is a sparsifying operator: we will assume it to be a square wavelet transform.
- $\|\cdot\|_{\mathrm{TV}}$ is the Total Variation (TV) norm.

Sparse MRI

$$\min_{\boldsymbol{x}} \frac{1}{2}\|\mathcal{F}_u\boldsymbol{x} - \boldsymbol{y}\|_2^2 + \rho_1\|\boldsymbol{\Phi}\boldsymbol{x}\|_1 + \rho_2\|\boldsymbol{x}\|_{\mathrm{TV}}.$$

- $\boldsymbol{x} \in \mathbb{C}^N$ is the reconstructed MR image in vectorized form.
- $\mathcal{F}_u$ is the undersampled Fourier transform operator: conversion from the vectorized image to the k-space.
- $\boldsymbol{y} = \mathcal{F}_u\boldsymbol{x}^\star + \boldsymbol{\eta} \in \mathbb{C}^\kappa$ is the observation vector in the k-space.
- $\boldsymbol{x}^\star$ is the true underlying image and $\boldsymbol{\eta}$ is the additive noise.
- The ratio κ/N quantifies the undersampling.
- $\|\cdot\|_1$ denotes the ℓ_1 norm.
- $\boldsymbol{\Phi}$ is a sparsifying operator: we will assume it to be a square wavelet transform.
- $\|\cdot\|_{\mathrm{TV}}$ is the Total Variation (TV) norm.

Sparse MRI

$$\min_{\boldsymbol{x}} \frac{1}{2}\|\mathcal{F}_u \boldsymbol{x} - \boldsymbol{y}\|_2^2 + \rho_1 \|\boldsymbol{\Phi x}\|_1 + \rho_2 \|\boldsymbol{x}\|_{\mathrm{TV}}.$$

- $\boldsymbol{x} \in \mathbb{C}^N$ is the reconstructed MR image in vectorized form.
- $\mathcal{F}_u$ is the undersampled Fourier transform operator: conversion from the vectorized image to the k-space.
- $\boldsymbol{y} = \mathcal{F}_u \boldsymbol{x}^\star + \boldsymbol{\eta} \in \mathbb{C}^\kappa$ is the observation vector in the k-space.
- $\boldsymbol{x}^\star$ is the true underlying image and $\boldsymbol{\eta}$ is the additive noise.
- The ratio κ/N quantifies the undersampling.
- $\|\cdot\|_1$ denotes the ℓ_1 norm.
- $\boldsymbol{\Phi}$ is a sparsifying operator: we will assume it to be a square wavelet transform.
- $\|\cdot\|_{\mathrm{TV}}$ is the Total Variation (TV) norm.

Sparse MRI

$$\min_{\boldsymbol{x}} \frac{1}{2}\|\mathcal{F}_u\boldsymbol{x} - \boldsymbol{y}\|_2^2 + \rho_1\|\boldsymbol{\Phi}\boldsymbol{x}\|_1 + \rho_2\|\boldsymbol{x}\|_{\mathrm{TV}}.$$

- $\boldsymbol{x} \in \mathbb{C}^N$ is the reconstructed MR image in vectorized form.
- $\mathcal{F}_u$ is the undersampled Fourier transform operator: conversion from the vectorized image to the k-space.
- $\boldsymbol{y} = \mathcal{F}_u\boldsymbol{x}^\star + \boldsymbol{\eta} \in \mathbb{C}^\kappa$ is the observation vector in the k-space.
- $\boldsymbol{x}^\star$ is the true underlying image and $\boldsymbol{\eta}$ is the additive noise.
- The ratio κ/N quantifies the undersampling.
- $\|\cdot\|_1$ denotes the ℓ_1 norm.
- $\boldsymbol{\Phi}$ is a sparsifying operator: we will assume it to be a square wavelet transform.
- $\|\cdot\|_{\mathrm{TV}}$ is the Total Variation (TV) norm.

Sparse MRI

$$\min_{\boldsymbol{x}} \frac{1}{2}\|\mathcal{F}_u\boldsymbol{x} - \boldsymbol{y}\|_2^2 + \rho_1\|\boldsymbol{\Phi}\boldsymbol{x}\|_1 + \rho_2\|\boldsymbol{x}\|_{\mathrm{TV}}.$$

- $\boldsymbol{x} \in \mathbb{C}^N$ is the reconstructed MR image in vectorized form.
- $\mathcal{F}_u$ is the undersampled Fourier transform operator: conversion from the vectorized image to the k-space.
- $\boldsymbol{y} = \mathcal{F}_u\boldsymbol{x}^\star + \boldsymbol{\eta} \in \mathbb{C}^\kappa$ is the observation vector in the k-space.
- $\boldsymbol{x}^\star$ is the true underlying image and $\boldsymbol{\eta}$ is the additive noise.
- The ratio κ/N quantifies the undersampling.
- $\|\cdot\|_1$ denotes the ℓ_1 norm.
- $\boldsymbol{\Phi}$ is a sparsifying operator: we will assume it to be a square wavelet transform.
- $\|\cdot\|_{\mathrm{TV}}$ is the Total Variation (TV) norm.

Sparse MRI

$$\min_{\boldsymbol{x}} \frac{1}{2}\|\mathcal{F}_u \boldsymbol{x} - \boldsymbol{y}\|_2^2 + \rho_1 \|\boldsymbol{\Phi} \boldsymbol{x}\|_1 + \rho_2 \|\boldsymbol{x}\|_{\mathrm{TV}}.$$

- $\boldsymbol{x} \in \mathbb{C}^N$ is the reconstructed MR image in vectorized form.
- $\mathcal{F}_u$ is the undersampled Fourier transform operator: conversion from the vectorized image to the k-space.
- $\boldsymbol{y} = \mathcal{F}_u \boldsymbol{x}^\star + \boldsymbol{\eta} \in \mathbb{C}^\kappa$ is the observation vector in the k-space.
- $\boldsymbol{x}^\star$ is the true underlying image and $\boldsymbol{\eta}$ is the additive noise.
- The ratio κ/N quantifies the undersampling.
- $\|\cdot\|_1$ denotes the ℓ_1 norm.
- $\boldsymbol{\Phi}$ is a sparsifying operator: we will assume it to be a square wavelet transform.
- $\|\cdot\|_{\mathrm{TV}}$ is the Total Variation (TV) norm.

Outline

1. Introduction
   - The Problem
   - The Novel Approach
2. Transform Learning MRI
3. GTLMRI
   - New Cost
   - GTLMRI: Denoising
   - GTLMRI: Reconstruction
   - GTLMRI: Overall Algorithm
4. Simulations and Conclusion

Patch based regularization methods

- Examplar or patch based methods have been very popular for sparsity based image processing.
- Dictionary learning (DL) based synthesis sparsity methods
- Analysis sparsity based analysis operator learning methods
- Novel model for analysis operator learning, called as sparsifying Transform Learning (TL) [Ravishankar and Bresler, 2013].
- TL has been utilized to regularize the MRI reconstruction problem, resulting in the TLMRI algorithm.

Patch based regularization methods

- Examplar or patch based methods have been very popular for sparsity based image processing.
- Dictionary learning (DL) based synthesis sparsity methods
- Analysis sparsity based analysis operator learning methods
- Novel model for analysis operator learning, called as sparsifying Transform Learning (TL) [Ravishankar and Bresler, 2013].
- TL has been utilized to regularize the MRI reconstruction problem, resulting in the TLMRI algorithm.

Patch based regularization methods

- Examplar or patch based methods have been very popular for sparsity based image processing.
- Dictionary learning (DL) based synthesis sparsity methods
- Analysis sparsity based analysis operator learning methods
- Novel model for analysis operator learning, called as sparsifying Transform Learning (TL) [Ravishankar and Bresler, 2013].
- TL has been utilized to regularize the MRI reconstruction problem, resulting in the TLMRI algorithm.

Patch based regularization methods

- Examplar or patch based methods have been very popular for sparsity based image processing.
- Dictionary learning (DL) based synthesis sparsity methods
- Analysis sparsity based analysis operator learning methods
- Novel model for analysis operator learning, called as sparsifying Transform Learning (TL) [Ravishankar and Bresler, 2013].
- TL has been utilized to regularize the MRI reconstruction problem, resulting in the TLMRI algorithm.

Patch based regularization methods

- Examplar or patch based methods have been very popular for sparsity based image processing.
- Dictionary learning (DL) based synthesis sparsity methods
- Analysis sparsity based analysis operator learning methods
- Novel model for analysis operator learning, called as sparsifying Transform Learning (TL) [Ravishankar and Bresler, 2013].
- TL has been utilized to regularize the MRI reconstruction problem, resulting in the TLMRI algorithm.

Patch based regularization methods

- Methods such as Sparse MRI, RecPF and FCSA apply global, image-scale regularization
- TLMRI or DL based algorithms utilize local, patch-scale regularization
- In this work, we aim to bring these two ends together.

Patch based regularization methods

- Methods such as Sparse MRI, RecPF and FCSA apply global, image-scale regularization
- TLMRI or DL based algorithms utilize local, patch-scale regularization
- In this work, we aim to bring these two ends together.

Patch based regularization methods

- Methods such as Sparse MRI, RecPF and FCSA apply global, image-scale regularization
- TLMRI or DL based algorithms utilize local, patch-scale regularization
- In this work, we aim to bring these two ends together.

New Method: Globally regularized TLMRI

G-TLMRI

- We introduce a global sparsifying cost into TLMRI, and provide the algorithm.
- We will denote this modified framework as the Globally regularized TLMRI (G-TLMRI).
- Simulation results: use of global and local regularization terms together results in superior reconstruction performance.

New Method: Globally regularized TLMRI

G-TLMRI

- We introduce a global sparsifying cost into TLMRI, and provide the algorithm.
- We will denote this modified framework as the Globally regularized TLMRI (G-TLMRI).
- Simulation results: use of global and local regularization terms together results in superior reconstruction performance.

New Method: Globally regularized TLMRI

G-TLMRI

- We introduce a global sparsifying cost into TLMRI, and provide the algorithm.
- We will denote this modified framework as the Globally regularized TLMRI (G-TLMRI).
- Simulation results: use of global and local regularization terms together results in superior reconstruction performance.

From the Literature: Transform Learning MRI

TLMRI

- TL has been applied to MRI image reconstruction.
- TLMRI cost function can be stated as follows.

$$(\text{P0}) \quad \min_{\boldsymbol{W}, \hat{\mathcal{X}}, \mathcal{A}, \boldsymbol{x}} \; \|\boldsymbol{W}\hat{\mathcal{X}} - \mathcal{A}\|_F^2 + \lambda Q(\boldsymbol{W}) + \tau \|\mathcal{R}(\boldsymbol{x}) - \hat{\mathcal{X}}\|_F^2$$

$$+ \eta \|\mathcal{F}_u \boldsymbol{x} - \boldsymbol{y}\|_2^2 \, , \qquad \text{s.t. } \|\alpha_j\|_0 \leq s_j \; \forall j = 1 \dots M. \quad (2)$$

From the Literature: Transform Learning MRI
TLMRI

- TL has been applied to MRI image reconstruction.
- TLMRI cost function can be stated as follows.

$$(\text{P0}) \quad \min_{\boldsymbol{W},\hat{\mathcal{X}},\mathcal{A},\boldsymbol{x}} \|\boldsymbol{W}\hat{\mathcal{X}} - \mathcal{A}\|_F^2 + \lambda Q(\boldsymbol{W}) + \tau\|\mathcal{R}(\boldsymbol{x}) - \hat{\mathcal{X}}\|_F^2 + \eta\|\mathcal{F}_u\boldsymbol{x} - \boldsymbol{y}\|_2^2 , \quad \text{s.t.} \ \|\alpha_j\|_0 \leq s_j \ \forall j = 1 \dots M. \quad (2)$$

From the Literature: Transform Learning MRI
TLMRI

- TL has been applied to MRI image reconstruction.
- TLMRI cost function can be stated as follows.

$$\text{(P0)} \quad \min_{W,\hat{\mathcal{X}},\mathcal{A},x} \|W\hat{\mathcal{X}} - \mathcal{A}\|_F^2 + \lambda Q(W) + \tau\|\mathcal{R}(x) - \hat{\mathcal{X}}\|_F^2 + \eta\|\mathcal{F}_u x - y\|_2^2 , \quad \text{s.t. } \|\alpha_j\|_0 \leq s_j \ \forall j = 1 \ldots M. \quad (2)$$

From the Literature: Transform Learning MRI
TLMRI

- TL has been applied to MRI image reconstruction.
- TLMRI cost function can be stated as follows.

$$\text{(P0)} \quad \min_{\boldsymbol{W},\hat{\boldsymbol{\mathcal{X}}},\boldsymbol{\mathcal{A}},\boldsymbol{x}} \|\boldsymbol{W}\hat{\boldsymbol{\mathcal{X}}} - \boldsymbol{\mathcal{A}}\|_F^2 + \lambda Q(\boldsymbol{W}) + \tau\|\mathcal{R}(\boldsymbol{x}) - \hat{\boldsymbol{\mathcal{X}}}\|_F^2$$
$$+ \eta\|\mathcal{F}_u\boldsymbol{x} - \boldsymbol{y}\|_2^2 , \quad \text{s.t.} \ \|\alpha_j\|_0 \leq s_j \ \forall j = 1 \ldots M. \quad (2)$$

From the Literature: Transform Learning MRI
TLMRI

$$(\text{P0}) \quad \min_{\boldsymbol{W}, \hat{\mathcal{X}}, \mathcal{A}, \boldsymbol{x}} \|\boldsymbol{W}\hat{\mathcal{X}} - \mathcal{A}\|_F^2 + \lambda Q(\boldsymbol{W}) + \tau \|\mathcal{R}(\boldsymbol{x}) - \hat{\mathcal{X}}\|_F^2 + \eta \|\mathcal{F}_u \boldsymbol{x} - \boldsymbol{y}\|_2^2 , \quad \text{s.t. } \|\alpha_j\|_0 \leq s_j \ \forall j = 1 \ldots M.$$

- $\|\cdot\|_F$ is the Frobenius matrix norm.
- $\|\cdot\|_0$ denotes the ℓ_0 pseudo-norm.
- $\boldsymbol{W} \in \mathbb{C}^{n \times n}$ is the learned square transform.
- $\hat{\mathcal{X}} \in \mathbb{C}^{n \times M}$, and its columns $\hat{\boldsymbol{x}}_j \in \mathbb{C}^n$ denote vectorized 2D patches of size $\sqrt{n} \times \sqrt{n}$.

From the Literature: Transform Learning MRI
TLMRI

$$
\text{(P0)} \quad \min_{\boldsymbol{W}, \hat{\mathcal{X}}, \mathcal{A}, \boldsymbol{x}} \|\boldsymbol{W}\hat{\mathcal{X}} - \mathcal{A}\|_F^2 + \lambda Q(\boldsymbol{W}) + \tau \|\mathcal{R}(\boldsymbol{x}) - \hat{\mathcal{X}}\|_F^2 + \eta \|\mathcal{F}_u \boldsymbol{x} - \boldsymbol{y}\|_2^2 \,, \quad \text{s.t.} \;\; \|\alpha_j\|_0 \leq s_j \; \forall j = 1 \ldots M.
$$

- $\|\cdot\|_F$ is the Frobenius matrix norm.
- $\|\cdot\|_0$ denotes the ℓ_0 pseudo-norm.
- $\boldsymbol{W} \in \mathbb{C}^{n \times n}$ is the learned square transform.
- $\hat{\mathcal{X}} \in \mathbb{C}^{n \times M}$, and its columns $\hat{x}_j \in \mathbb{C}^n$ denote vectorized 2D patches of size $\sqrt{n} \times \sqrt{n}$.

From the Literature: Transform Learning MRI
TLMRI

$$\text{(P0)} \quad \min_{\boldsymbol{W}, \hat{\mathcal{X}}, \mathcal{A}, \boldsymbol{x}} \|\boldsymbol{W}\hat{\mathcal{X}} - \mathcal{A}\|_F^2 + \lambda Q(\boldsymbol{W}) + \tau \|\mathcal{R}(\boldsymbol{x}) - \hat{\mathcal{X}}\|_F^2 + \eta \|\mathcal{F}_u \boldsymbol{x} - \boldsymbol{y}\|_2^2, \quad \text{s.t. } \|\alpha_j\|_0 \leq s_j \; \forall j = 1 \ldots M.$$

- $\|\cdot\|_F$ is the Frobenius matrix norm.
- $\|\cdot\|_0$ denotes the ℓ_0 pseudo-norm.
- $\boldsymbol{W} \in \mathbb{C}^{n \times n}$ is the learned square transform.
- $\hat{\mathcal{X}} \in \mathbb{C}^{n \times M}$, and its columns $\hat{\boldsymbol{x}}_j \in \mathbb{C}^n$ denote vectorized 2D patches of size $\sqrt{n} \times \sqrt{n}$.

From the Literature: Transform Learning MRI

TLMRI

$$(\text{P0}) \quad \min_{\boldsymbol{W},\hat{\mathcal{X}},\mathcal{A},\boldsymbol{x}} \|\boldsymbol{W}\hat{\mathcal{X}} - \mathcal{A}\|_F^2 + \lambda Q(\boldsymbol{W}) + \tau \|\mathcal{R}(\boldsymbol{x}) - \hat{\mathcal{X}}\|_F^2 + \eta \|\mathcal{F}_u \boldsymbol{x} - \boldsymbol{y}\|_2^2 \,, \quad \text{s.t.} \; \|\alpha_j\|_0 \leq s_j \; \forall j = 1 \ldots M.$$

- $\|\cdot\|_F$ is the Frobenius matrix norm.
- $\|\cdot\|_0$ denotes the ℓ_0 pseudo-norm.
- $\boldsymbol{W} \in \mathbb{C}^{n \times n}$ is the learned square transform.
- $\hat{\mathcal{X}} \in \mathbb{C}^{n \times M}$, and its columns $\hat{\boldsymbol{x}}_j \in \mathbb{C}^n$ denote vectorized 2D patches of size $\sqrt{n} \times \sqrt{n}$.

From the Literature: Transform Learning MRI
TLMRI

$$\text{(P0)} \quad \min_{\boldsymbol{W},\hat{\mathcal{X}},\mathcal{A},\boldsymbol{x}} \|\boldsymbol{W}\hat{\mathcal{X}} - \mathcal{A}\|_F^2 + \lambda Q(\boldsymbol{W}) + \tau\|\mathcal{R}(\boldsymbol{x}) - \hat{\mathcal{X}}\|_F^2 + \eta\|\mathcal{F}_u\boldsymbol{x} - \boldsymbol{y}\|_2^2 , \quad \text{s.t.} \ \|\alpha_j\|_0 \leq s_j \ \forall j = 1 \ldots M.$$

- $\|\cdot\|_F$ is the Frobenius matrix norm.
- $\|\cdot\|_0$ denotes the ℓ_0 pseudo-norm.
- $\boldsymbol{W} \in \mathbb{C}^{n\times n}$ is the learned square transform.
- $\hat{\mathcal{X}} \in \mathbb{C}^{n\times M}$, and its columns $\hat{\boldsymbol{x}}_j \in \mathbb{C}^n$ denote vectorized 2D patches of size $\sqrt{n} \times \sqrt{n}$.

From the Literature: Transform Learning MRI

TLMRI

$$\text{(P0)} \quad \min_{\boldsymbol{W},\hat{\mathcal{X}},\mathcal{A},\boldsymbol{x}} \|\boldsymbol{W}\hat{\mathcal{X}} - \mathcal{A}\|_F^2 + \lambda Q(\boldsymbol{W}) + \tau \|\mathcal{R}(\boldsymbol{x}) - \hat{\mathcal{X}}\|_F^2 + \eta \|\mathcal{F}_u \boldsymbol{x} - \boldsymbol{y}\|_2^2 , \quad \text{s.t. } \|\boldsymbol{\alpha}_j\|_0 \leq s_j \ \forall j = 1 \ldots M.$$

- $\|\cdot\|_F$ is the Frobenius matrix norm.
- $\|\cdot\|_0$ denotes the ℓ_0 pseudo-norm.
- $\boldsymbol{W} \in \mathbb{C}^{n \times n}$ is the learned square transform.
- $\hat{\mathcal{X}} \in \mathbb{C}^{n \times M}$, and its columns $\hat{\boldsymbol{x}}_j \in \mathbb{C}^n$ denote vectorized 2D patches of size $\sqrt{n} \times \sqrt{n}$.

From the Literature: Transform Learning MRI
TLMRI

$$\text{(P0)} \quad \min_{W,\hat{\mathcal{X}},\mathcal{A},x} \|W\hat{\mathcal{X}} - \mathcal{A}\|_F^2 + \lambda Q(W) + \tau\|\mathcal{R}(x) - \hat{\mathcal{X}}\|_F^2 + \eta\|\mathcal{F}_u x - y\|_2^2\,, \quad \text{s.t. } \|\alpha_j\|_0 \leq s_j \; \forall j = 1\ldots M.$$

- $\mathcal{A} \in \mathbb{C}^{n \times M}$ includes the sparse codes.
- $Q(\cdot)$ penalization term for the learned W.
- $\mathcal{R}$ image to patch operator.
- Observation fidelity is enforced using the $\|\mathcal{F}_u x - y\|_2^2$ term.

From the Literature: Transform Learning MRI

TLMRI

$$\text{(P0)} \quad \min_{\boldsymbol{W}, \hat{\mathcal{X}}, \mathcal{A}, \boldsymbol{x}} \|\boldsymbol{W}\hat{\mathcal{X}} - \mathcal{A}\|_F^2 + \lambda Q(\boldsymbol{W}) + \tau \|\mathcal{R}(\boldsymbol{x}) - \hat{\mathcal{X}}\|_F^2 + \eta \|\mathcal{F}_u \boldsymbol{x} - \boldsymbol{y}\|_2^2 , \quad \text{s.t. } \|\alpha_j\|_0 \leq s_j \ \forall j = 1 \ldots M.$$

- $\mathcal{A} \in \mathbb{C}^{n \times M}$ includes the sparse codes.
- $Q(\cdot)$ penalization term for the learned $\boldsymbol{W}$.
- $\mathcal{R}$ image to patch operator.
- Observation fidelity is enforced using the $\|\mathcal{F}_u \boldsymbol{x} - \boldsymbol{y}\|_2^2$ term.

From the Literature: Transform Learning MRI
TLMRI

$$
\text{(P0)} \quad \min_{\boldsymbol{W}, \hat{\mathcal{X}}, \mathcal{A}, \boldsymbol{x}} \|\boldsymbol{W}\hat{\mathcal{X}} - \mathcal{A}\|_F^2 + \lambda Q(\boldsymbol{W}) + \tau \|\mathcal{R}(\boldsymbol{x}) - \hat{\mathcal{X}}\|_F^2 + \eta \|\mathcal{F}_u \boldsymbol{x} - \boldsymbol{y}\|_2^2 , \quad \text{s.t.} \ \|\alpha_j\|_0 \le s_j \ \forall j = 1 \ldots M.
$$

- $\mathcal{A} \in \mathbb{C}^{n \times M}$ includes the sparse codes.
- $Q(\cdot)$ penalization term for the learned $\boldsymbol{W}$.
- $\mathcal{R}$ image to patch operator.
- Observation fidelity is enforced using the $\|\mathcal{F}_u \boldsymbol{x} - \boldsymbol{y}\|_2^2$ term.

From the Literature: Transform Learning MRI
TLMRI

$$\text{(P0)} \quad \min_{\boldsymbol{W}, \hat{\mathcal{X}}, \mathcal{A}, \boldsymbol{x}} \|\boldsymbol{W}\hat{\mathcal{X}} - \mathcal{A}\|_F^2 + \lambda Q(\boldsymbol{W}) + \tau \|\mathcal{R}(\boldsymbol{x}) - \hat{\mathcal{X}}\|_F^2$$
$$+ \eta \|\mathcal{F}_u \boldsymbol{x} - \boldsymbol{y}\|_2^2 , \quad \text{s.t.} \ \|\alpha_j\|_0 \leq s_j \ \forall j = 1 \ldots M.$$

- $\mathcal{A} \in \mathbb{C}^{n \times M}$ includes the sparse codes.
- $Q(\cdot)$ penalization term for the learned $\boldsymbol{W}$.
- $\mathcal{R}$ image to patch operator.
- Observation fidelity is enforced using the $\|\mathcal{F}_u \boldsymbol{x} - \boldsymbol{y}\|_2^2$ term.

From the Literature: Transform Learning MRI

TLMRI

$$\text{(P0)} \quad \min_{\boldsymbol{W},\hat{\mathcal{X}},\mathcal{A},\boldsymbol{x}} \|\boldsymbol{W}\hat{\mathcal{X}} - \mathcal{A}\|_F^2 + \lambda Q(\boldsymbol{W}) + \tau \|\mathcal{R}(\boldsymbol{x}) - \hat{\mathcal{X}}\|_F^2 + \eta \|\mathcal{F}_u \boldsymbol{x} - \boldsymbol{y}\|_2^2 , \quad \text{s.t. } \|\alpha_j\|_0 \leq s_j \ \forall j = 1 \ldots M.$$

- $\mathcal{A} \in \mathbb{C}^{n \times M}$ includes the sparse codes.
- $Q(\cdot)$ penalization term for the learned $\boldsymbol{W}$.
- $\mathcal{R}$ image to patch operator.
- Observation fidelity is enforced using the $\|\mathcal{F}_u \boldsymbol{x} - \boldsymbol{y}\|_2^2$ term.

From the Literature: Transform Learning MRI
TLMRI

$$\text{(P0)} \quad \min_{\boldsymbol{W}, \hat{\mathcal{X}}, \mathcal{A}, \boldsymbol{x}} \|\boldsymbol{W}\hat{\mathcal{X}} - \mathcal{A}\|_F^2 + \lambda Q(\boldsymbol{W}) + \tau \|\mathcal{R}(\boldsymbol{x}) - \hat{\mathcal{X}}\|_F^2 + \eta \|\mathcal{F}_u \boldsymbol{x} - \boldsymbol{y}\|_2^2, \quad \text{s.t. } \|\alpha_j\|_0 \leq s_j \; \forall j = 1 \ldots M.$$

- $\mathcal{A} \in \mathbb{C}^{n \times M}$ includes the sparse codes.
- $Q(\cdot)$ penalization term for the learned $\boldsymbol{W}$.
- $\mathcal{R}$ image to patch operator.
- Observation fidelity is enforced using the $\|\mathcal{F}_u \boldsymbol{x} - \boldsymbol{y}\|_2^2$ term.

From the Literature: Transform Learning MRI
TLMRI

- TLMRI applies local regularization via a learned sparsifying transform.
- TLMRI with learned, local regularization: good performance when compared to nonadaptive global regularization (such as wavelet plus TV regularization in Sparse MRI).
- In this work: include additional global regularization in the TLMRI framework.

From the Literature: Transform Learning MRI
TLMRI

- TLMRI applies local regularization via a learned sparsifying transform.
- TLMRI with learned, local regularization: good performance when compared to nonadaptive global regularization (such as wavelet plus TV regularization in Sparse MRI).
- In this work: include additional global regularization in the TLMRI framework.

From the Literature: Transform Learning MRI

TLMRI

- TLMRI applies local regularization via a learned sparsifying transform.
- TLMRI with learned, local regularization: good performance when compared to nonadaptive global regularization (such as wavelet plus TV regularization in Sparse MRI).
- In this work: include additional global regularization in the TLMRI framework.

Outline

1. Introduction
   - The Problem
   - The Novel Approach
2. Transform Learning MRI
3. GTLMRI
   - New Cost
   - GTLMRI: Denoising
   - GTLMRI: Reconstruction
   - GTLMRI: Overall Algorithm
4. Simulations and Conclusion

New Method: GTLMRI

- New cost function with global regularizer.

$$
\text{(P1)} \quad \min_{\boldsymbol{W},\hat{\mathcal{X}},\mathcal{A},\boldsymbol{x}} \|\boldsymbol{W}\hat{\mathcal{X}} - \mathcal{A}\|_F^2 + \lambda Q(\boldsymbol{W}) + \beta\|\mathcal{A}\|_1 + \tau\|\mathcal{R}(\boldsymbol{x}) - \hat{\mathcal{X}}\|_F^2 + \eta\|\mathcal{F}_u\boldsymbol{x} - \boldsymbol{y}\|_2^2 + \upsilon'\|\boldsymbol{\Phi x}\|_1. \quad (3)
$$

New Method: GTLMRI

- New cost function with global regularizer.

$$\text{(P1)} \quad \min_{\boldsymbol{W},\hat{\mathcal{X}},\mathcal{A},\boldsymbol{x}} \|\boldsymbol{W}\hat{\mathcal{X}} - \mathcal{A}\|_F^2 + \lambda Q(\boldsymbol{W}) + \beta\|\mathcal{A}\|_1$$
$$+ \tau\|\mathcal{R}(\boldsymbol{x}) - \hat{\mathcal{X}}\|_F^2 + \eta\|\mathcal{F}_u\boldsymbol{x} - \boldsymbol{y}\|_2^2 + \upsilon'\|\boldsymbol{\Phi x}\|_1. \quad (3)$$

New Method: GTLMRI

- New cost function with global regularizer.

$$\text{(P1)} \quad \min_{\boldsymbol{W},\hat{\boldsymbol{\mathcal{X}}},\boldsymbol{\mathcal{A}},\boldsymbol{x}} \|\boldsymbol{W}\hat{\boldsymbol{\mathcal{X}}} - \boldsymbol{\mathcal{A}}\|_F^2 + \lambda Q(\boldsymbol{W}) + \beta\|\boldsymbol{\mathcal{A}}\|_1 + \tau\|\mathcal{R}(\boldsymbol{x}) - \hat{\boldsymbol{\mathcal{X}}}\|_F^2 + \eta\|\mathcal{F}_u\boldsymbol{x} - \boldsymbol{y}\|_2^2 + \upsilon'\|\boldsymbol{\Phi}\boldsymbol{x}\|_1. \quad (3)$$

New Method: GTLMRI

$$\text{(P1)} \quad \min_{W,\hat{\mathcal{X}},\mathcal{A},x} \|W\hat{\mathcal{X}} - \mathcal{A}\|_F^2 + \lambda Q(W) + \beta\|\mathcal{A}\|_1 + \tau\|\mathcal{R}(x) - \hat{\mathcal{X}}\|_F^2 + \eta\|\mathcal{F}_u x - y\|_2^2 + \upsilon'\|\Phi x\|_1 .$$

$$\text{(P0)} \quad \min_{W,\hat{\mathcal{X}},\mathcal{A},x} \|W\hat{\mathcal{X}} - \mathcal{A}\|_F^2 + \lambda Q(W) + \tau\|\mathcal{R}(x) - \hat{\mathcal{X}}\|_F^2 + \eta\|\mathcal{F}_u x - y\|_2^2 , \quad \text{s.t. } \|\alpha_j\|_0 \le s_j \; \forall j = 1 \dots M.$$

- When compared with (P0), in (P1) the crucial change is the introduction of the $\|\Phi x\|_1$ term.
- We will denote this modified framework as the Globally regularized TLMRI (G-TLMRI).

New Method: GTLMRI

$$\text{(P1)} \quad \min_{\boldsymbol{W}, \hat{\mathcal{X}}, \mathcal{A}, \boldsymbol{x}} \|\boldsymbol{W}\hat{\mathcal{X}} - \mathcal{A}\|_F^2 + \lambda Q(\boldsymbol{W}) + \beta\|\mathcal{A}\|_1 + \tau\|\mathcal{R}(\boldsymbol{x}) - \hat{\mathcal{X}}\|_F^2 + \eta\|\mathcal{F}_u\boldsymbol{x} - \boldsymbol{y}\|_2^2 + \upsilon'\|\boldsymbol{\Phi}\boldsymbol{x}\|_1.$$

$$\text{(P0)} \quad \min_{\boldsymbol{W}, \hat{\mathcal{X}}, \mathcal{A}, \boldsymbol{x}} \|\boldsymbol{W}\hat{\mathcal{X}} - \mathcal{A}\|_F^2 + \lambda Q(\boldsymbol{W}) + \tau\|\mathcal{R}(\boldsymbol{x}) - \hat{\mathcal{X}}\|_F^2 + \eta\|\mathcal{F}_u\boldsymbol{x} - \boldsymbol{y}\|_2^2, \quad \text{s.t. } \|\alpha_j\|_0 \leq s_j \ \forall j = 1 \ldots M.$$

- When compared with (P0), in (P1) the crucial change is the introduction of the $\|\boldsymbol{\Phi}\boldsymbol{x}\|_1$ term.
- We will denote this modified framework as the Globally regularized TLMRI (G-TLMRI).

New Method: GTLMRI

$$\text{(P1)} \quad \min_{\boldsymbol{W},\hat{\mathcal{X}},\mathcal{A},\boldsymbol{x}} \|\boldsymbol{W}\hat{\mathcal{X}} - \mathcal{A}\|_F^2 + \lambda Q(\boldsymbol{W}) + \beta\|\mathcal{A}\|_1 + \tau\|\mathcal{R}(\boldsymbol{x}) - \hat{\mathcal{X}}\|_F^2 + \eta\|\mathcal{F}_u\boldsymbol{x} - \boldsymbol{y}\|_2^2 + \upsilon'\|\boldsymbol{\Phi}\boldsymbol{x}\|_1.$$

$$\text{(P0)} \quad \min_{\boldsymbol{W},\hat{\mathcal{X}},\mathcal{A},\boldsymbol{x}} \|\boldsymbol{W}\hat{\mathcal{X}} - \mathcal{A}\|_F^2 + \lambda Q(\boldsymbol{W}) + \tau\|\mathcal{R}(\boldsymbol{x}) - \hat{\mathcal{X}}\|_F^2 + \eta\|\mathcal{F}_u\boldsymbol{x} - \boldsymbol{y}\|_2^2, \quad \text{s.t. } \|\alpha_j\|_0 \leq s_j \ \forall j = 1 \ldots M.$$

- When compared with (P0), in (P1) the crucial change is the introduction of the $\|\boldsymbol{\Phi x}\|_1$ term.
- We will denote this modified framework as the Globally regularized TLMRI (G-TLMRI).

New Method: GTLMRI

$$\text{(P1)} \quad \min_{\boldsymbol{W},\hat{\mathcal{X}},\mathcal{A},\boldsymbol{x}} \|\boldsymbol{W}\hat{\mathcal{X}} - \mathcal{A}\|_F^2 + \lambda Q(\boldsymbol{W}) + \beta\|\mathcal{A}\|_1 + \tau\|\mathcal{R}(\boldsymbol{x}) - \hat{\mathcal{X}}\|_F^2 + \eta\|\mathcal{F}_u\boldsymbol{x} - \boldsymbol{y}\|_2^2 + \upsilon'\|\boldsymbol{\Phi x}\|_1.$$

$$\text{(P0)} \quad \min_{\boldsymbol{W},\hat{\mathcal{X}},\mathcal{A},\boldsymbol{x}} \|\boldsymbol{W}\hat{\mathcal{X}} - \mathcal{A}\|_F^2 + \lambda Q(\boldsymbol{W}) + \tau\|\mathcal{R}(\boldsymbol{x}) - \hat{\mathcal{X}}\|_F^2 + \eta\|\mathcal{F}_u\boldsymbol{x} - \boldsymbol{y}\|_2^2, \quad \text{s.t.} \ \|\alpha_j\|_0 \le s_j \ \forall j = 1 \dots M.$$

- When compared with (P0), in (P1) the crucial change is the introduction of the $\|\boldsymbol{\Phi x}\|_1$ term.
- We will denote this modified framework as the Globally regularized TLMRI (G-TLMRI).

New Method: GTLMRI

$$\text{(P1)} \quad \min_{\boldsymbol{W},\hat{\mathcal{X}},\mathcal{A},\boldsymbol{x}} \|\boldsymbol{W}\hat{\mathcal{X}} - \mathcal{A}\|_F^2 + \lambda Q(\boldsymbol{W}) + \beta\|\mathcal{A}\|_1 + \tau\|\mathcal{R}(\boldsymbol{x}) - \hat{\mathcal{X}}\|_F^2 + \eta\|\mathcal{F}_u\boldsymbol{x} - \boldsymbol{y}\|_2^2 + \upsilon'\|\boldsymbol{\Phi x}\|_1 .$$

$$\text{(P0)} \quad \min_{\boldsymbol{W},\hat{\mathcal{X}},\mathcal{A},\boldsymbol{x}} \|\boldsymbol{W}\hat{\mathcal{X}} - \mathcal{A}\|_F^2 + \lambda Q(\boldsymbol{W}) + \tau\|\mathcal{R}(\boldsymbol{x}) - \hat{\mathcal{X}}\|_F^2 + \eta\|\mathcal{F}_u\boldsymbol{x} - \boldsymbol{y}\|_2^2 , \quad \text{s.t.} \ \|\alpha_j\|_0 \leq s_j \ \forall j = 1 \ldots M.$$

- When compared with (P0), in (P1) the crucial change is the introduction of the $\|\boldsymbol{\Phi x}\|_1$ term.
- We will denote this modified framework as the Globally regularized TLMRI (G-TLMRI).

New Method: GTLMRI

- We will separate the algorithm into two steps with and without optimization on $\boldsymbol{x}$.

$$\text{(P2)} \min_{\boldsymbol{W},\hat{\mathcal{X}},\mathcal{A}} \|\boldsymbol{W}\hat{\mathcal{X}} - \mathcal{A}\|_F^2 + \lambda Q(\boldsymbol{W}) + \beta\|\mathcal{A}\|_1 + \tau\|\mathcal{R}(\boldsymbol{x}) - \hat{\mathcal{X}}\|_F^2. \quad (4)$$

$$\text{(P3)} \min_{\boldsymbol{x}} \frac{1}{2}\|\mathcal{F}_u\boldsymbol{x} - \boldsymbol{y}\|_2^2 + \frac{\tau}{2\eta}\|\mathcal{R}(\boldsymbol{x}) - \hat{\mathcal{X}}\|_F^2 + \frac{\upsilon'}{2\eta}\|\boldsymbol{\Phi x}\|_1. \quad (5)$$

- (P2) can be thought of as denoising.
- (P3) can be thought of as reconstruction.

New Method: GTLMRI

- We will separate the algorithm into two steps with and without optimization on $\boldsymbol{x}$.

$$\text{(P2)}\ \min_{\boldsymbol{W},\hat{\mathcal{X}},\mathcal{A}} \|\boldsymbol{W}\hat{\mathcal{X}}-\mathcal{A}\|_F^2+\lambda Q(\boldsymbol{W})+\beta\|\mathcal{A}\|_1+\tau\|\mathcal{R}(\boldsymbol{x})-\hat{\mathcal{X}}\|_F^2. \quad (4)$$

$$\text{(P3)}\ \min_{\boldsymbol{x}} \frac{1}{2}\|\mathcal{F}_u\boldsymbol{x}-\boldsymbol{y}\|_2^2+\frac{\tau}{2\eta}\|\mathcal{R}(\boldsymbol{x})-\hat{\mathcal{X}}\|_F^2+\frac{\upsilon'}{2\eta}\|\boldsymbol{\Phi x}\|_1. \quad (5)$$

- (P2) can be thought of as denoising.
- (P3) can be thought of as reconstruction.

New Method: GTLMRI

- We will separate the algorithm into two steps with and without optimization on $\boldsymbol{x}$.

$$\text{(P2)} \min_{\boldsymbol{W},\hat{\mathcal{X}},\mathcal{A}} \|\boldsymbol{W}\hat{\mathcal{X}}-\mathcal{A}\|_F^2+\lambda Q(\boldsymbol{W})+\beta\|\mathcal{A}\|_1+\tau\|\mathcal{R}(\boldsymbol{x})-\hat{\mathcal{X}}\|_F^2. \quad (4)$$

$$\text{(P3)} \min_{\boldsymbol{x}} \frac{1}{2}\|\mathcal{F}_u\boldsymbol{x}-\boldsymbol{y}\|_2^2+\frac{\tau}{2\eta}\|\mathcal{R}(\boldsymbol{x})-\hat{\mathcal{X}}\|_F^2+\frac{\upsilon'}{2\eta}\|\boldsymbol{\Phi}\boldsymbol{x}\|_1. \quad (5)$$

- (P2) can be thought of as denoising.
- (P3) can be thought of as reconstruction.

New Method: GTLMRI

- We will separate the algorithm into two steps with and without optimization on $\boldsymbol{x}$.

$$\text{(P2)} \min_{\boldsymbol{W},\hat{\mathcal{X}},\mathcal{A}} \|\boldsymbol{W}\hat{\mathcal{X}} - \mathcal{A}\|_F^2 + \lambda Q(\boldsymbol{W}) + \beta\|\mathcal{A}\|_1 + \tau\|\mathcal{R}(\boldsymbol{x}) - \hat{\mathcal{X}}\|_F^2. \quad (4)$$

$$\text{(P3)} \min_{\boldsymbol{x}} \frac{1}{2}\|\mathcal{F}_u\boldsymbol{x} - \boldsymbol{y}\|_2^2 + \frac{\tau}{2\eta}\|\mathcal{R}(\boldsymbol{x}) - \hat{\mathcal{X}}\|_F^2 + \frac{\upsilon'}{2\eta}\|\boldsymbol{\Phi}\boldsymbol{x}\|_1. \quad (5)$$

- (P2) can be thought of as denoising.
- (P3) can be thought of as reconstruction.

New Method: GTLMRI

- We will separate the algorithm into two steps with and without optimization on $\boldsymbol{x}$.

$$\text{(P2)} \min_{\boldsymbol{W},\hat{\mathcal{X}},\mathcal{A}} \|\boldsymbol{W}\hat{\mathcal{X}}-\mathcal{A}\|_F^2+\lambda Q(\boldsymbol{W})+\beta\|\mathcal{A}\|_1+\tau\|\mathcal{R}(\boldsymbol{x})-\hat{\mathcal{X}}\|_F^2. \quad (4)$$

$$\text{(P3)} \min_{\boldsymbol{x}} \frac{1}{2}\|\mathcal{F}_u\boldsymbol{x}-\boldsymbol{y}\|_2^2+\frac{\tau}{2\eta}\|\mathcal{R}(\boldsymbol{x})-\hat{\mathcal{X}}\|_F^2+\frac{\upsilon'}{2\eta}\|\boldsymbol{\Phi}\boldsymbol{x}\|_1. \quad (5)$$

- (P2) can be thought of as denoising.
- (P3) can be thought of as reconstruction.

New Method: GTLMRI

- We will separate the algorithm into two steps with and without optimization on $\boldsymbol{x}$.

$$\text{(P2)} \min_{\boldsymbol{W},\hat{\mathcal{X}},\mathcal{A}} \|\boldsymbol{W}\hat{\mathcal{X}} - \mathcal{A}\|_F^2 + \lambda Q(\boldsymbol{W}) + \beta\|\mathcal{A}\|_1 + \tau\|\mathcal{R}(\boldsymbol{x}) - \hat{\mathcal{X}}\|_F^2. \quad (4)$$

$$\text{(P3)} \min_{\boldsymbol{x}} \frac{1}{2}\|\mathcal{F}_u\boldsymbol{x} - \boldsymbol{y}\|_2^2 + \frac{\tau}{2\eta}\|\mathcal{R}(\boldsymbol{x}) - \hat{\mathcal{X}}\|_F^2 + \frac{\upsilon'}{2\eta}\|\boldsymbol{\Phi}\boldsymbol{x}\|_1. \quad (5)$$

- (P2) can be thought of as denoising.
- (P3) can be thought of as reconstruction.

Outline

1 Introduction
- The Problem
- The Novel Approach

2 Transform Learning MRI

3 GTLMRI
- New Cost
- GTLMRI: Denoising
- GTLMRI: Reconstruction
- GTLMRI: Overall Algorithm

4 Simulations and Conclusion

GTLMRI: Denoising

- We will divide (P2) into two in the following form similar to the TLMRI.

$$\text{(P2.1)} \min_{\boldsymbol{W},\mathcal{A}} \|\boldsymbol{W}\hat{\mathcal{X}} - \mathcal{A}\|_F^2 + \lambda Q(\boldsymbol{W}) + \beta\|\mathcal{A}\|_1.$$

$$\text{(P2.2)} \min_{\hat{\mathcal{X}},\mathcal{A}} \|\boldsymbol{W}\hat{\mathcal{X}} - \mathcal{A}\|_F^2 + \beta\|\mathcal{A}\|_1 + \tau\|\mathcal{R}(\boldsymbol{x}) - \hat{\mathcal{X}}\|_F^2.$$

GTLMRI: Denoising

- We will divide (P2) into two in the following form similar to the TLMRI.

$$\text{(P2.1)} \min_{\boldsymbol{W},\mathcal{A}} \|\boldsymbol{W}\hat{\mathcal{X}} - \mathcal{A}\|_F^2 + \lambda Q(\boldsymbol{W}) + \beta\|\mathcal{A}\|_1.$$

$$\text{(P2.2)} \min_{\hat{\mathcal{X}},\mathcal{A}} \|\boldsymbol{W}\hat{\mathcal{X}} - \mathcal{A}\|_F^2 + \beta\|\mathcal{A}\|_1 + \tau\|\mathcal{R}(\boldsymbol{x}) - \hat{\mathcal{X}}\|_F^2.$$

GTLMRI: Denoising

- We will divide (P2) into two in the following form similar to the TLMRI.

$$\text{(P2.1)} \min_{\boldsymbol{W},\boldsymbol{\mathcal{A}}} \|\boldsymbol{W}\hat{\boldsymbol{\mathcal{X}}} - \boldsymbol{\mathcal{A}}\|_F^2 + \lambda Q(\boldsymbol{W}) + \beta\|\boldsymbol{\mathcal{A}}\|_1 .$$

$$\text{(P2.2)} \min_{\hat{\boldsymbol{\mathcal{X}}},\boldsymbol{\mathcal{A}}} \|\boldsymbol{W}\hat{\boldsymbol{\mathcal{X}}} - \boldsymbol{\mathcal{A}}\|_F^2 + \beta\|\boldsymbol{\mathcal{A}}\|_1 + \tau\|\mathcal{R}(\boldsymbol{x}) - \hat{\boldsymbol{\mathcal{X}}}\|_F^2 .$$

GTLMRI: Denoising

- We will divide (P2) into two in the following form similar to the TLMRI.

$$\text{(P2.1)} \min_{\boldsymbol{W},\boldsymbol{\mathcal{A}}} \|\boldsymbol{W}\hat{\boldsymbol{\mathcal{X}}} - \boldsymbol{\mathcal{A}}\|_F^2 + \lambda Q(\boldsymbol{W}) + \beta\|\boldsymbol{\mathcal{A}}\|_1 .$$

$$\text{(P2.2)} \min_{\hat{\boldsymbol{\mathcal{X}}},\boldsymbol{\mathcal{A}}} \|\boldsymbol{W}\hat{\boldsymbol{\mathcal{X}}} - \boldsymbol{\mathcal{A}}\|_F^2 + \beta\|\boldsymbol{\mathcal{A}}\|_1 + \tau\|\boldsymbol{\mathcal{R}}(\boldsymbol{x}) - \hat{\boldsymbol{\mathcal{X}}}\|_F^2 .$$

GTLMRI: Denoising

- We will divide (P2) into two in the following form similar to the TLMRI.

$$\text{(P2.1)} \min_{\boldsymbol{W},\boldsymbol{\mathcal{A}}} \|\boldsymbol{W}\hat{\boldsymbol{\mathcal{X}}} - \boldsymbol{\mathcal{A}}\|_F^2 + \lambda Q(\boldsymbol{W}) + \beta\|\boldsymbol{\mathcal{A}}\|_1.$$

$$\text{(P2.2)} \min_{\hat{\boldsymbol{\mathcal{X}}},\boldsymbol{\mathcal{A}}} \|\boldsymbol{W}\hat{\boldsymbol{\mathcal{X}}} - \boldsymbol{\mathcal{A}}\|_F^2 + \beta\|\boldsymbol{\mathcal{A}}\|_1 + \tau\|\boldsymbol{\mathcal{R}}(\boldsymbol{x}) - \hat{\boldsymbol{\mathcal{X}}}\|_F^2.$$

GTLMRI: Denoising

- (P2.1) can be approximately solved using iterative alternation over two steps.

$$\text{(P2.1.1)} \min_{\mathcal{A}} \|\boldsymbol{W}\hat{\mathcal{X}} - \mathcal{A}\|_F^2 + \beta\|\mathcal{A}\|_1.$$

$$\text{(P2.1.2)} \min_{\boldsymbol{W}} \|\boldsymbol{W}\hat{\mathcal{X}} - \mathcal{A}\|_F^2 + \lambda Q(\boldsymbol{W}).$$

- Both (P2.1.1) and (P2.1.2) have closed form solutions.

GTLMRI: Denoising

- (P2.1) can be approximately solved using iterative alternation over two steps.

$$\text{(P2.1.1)} \min_{\mathcal{A}} \|\boldsymbol{W}\hat{\mathcal{X}} - \mathcal{A}\|_F^2 + \beta\|\mathcal{A}\|_1.$$

$$\text{(P2.1.2)} \min_{\boldsymbol{W}} \|\boldsymbol{W}\hat{\mathcal{X}} - \mathcal{A}\|_F^2 + \lambda Q(\boldsymbol{W}).$$

- Both (P2.1.1) and (P2.1.2) have closed form solutions.

GTLMRI: Denoising

- (P2.1) can be approximately solved using iterative alternation over two steps.

$$\text{(P2.1.1)} \min_{\mathcal{A}} \|\boldsymbol{W}\hat{\mathcal{X}} - \mathcal{A}\|_F^2 + \beta\|\mathcal{A}\|_1.$$

$$\text{(P2.1.2)} \min_{\boldsymbol{W}} \|\boldsymbol{W}\hat{\mathcal{X}} - \mathcal{A}\|_F^2 + \lambda Q(\boldsymbol{W}).$$

- Both (P2.1.1) and (P2.1.2) have closed form solutions.

GTLMRI: Denoising

- (P2.1) can be approximately solved using iterative alternation over two steps.

$$\text{(P2.1.1)} \min_{\mathcal{A}} \|\boldsymbol{W}\hat{\mathcal{X}} - \mathcal{A}\|_F^2 + \beta\|\mathcal{A}\|_1.$$

$$\text{(P2.1.2)} \min_{\boldsymbol{W}} \|\boldsymbol{W}\hat{\mathcal{X}} - \mathcal{A}\|_F^2 + \lambda Q(\boldsymbol{W}).$$

- Both (P2.1.1) and (P2.1.2) have closed form solutions.

GTLMRI: Denoising

- (P2.1) can be approximately solved using iterative alternation over two steps.

$$\text{(P2.1.1)}\ \min_{\boldsymbol{\mathcal{A}}} \|\boldsymbol{W}\hat{\boldsymbol{\mathcal{X}}} - \boldsymbol{\mathcal{A}}\|_F^2 + \beta\|\boldsymbol{\mathcal{A}}\|_1.$$

$$\text{(P2.1.2)}\ \min_{\boldsymbol{W}} \|\boldsymbol{W}\hat{\boldsymbol{\mathcal{X}}} - \boldsymbol{\mathcal{A}}\|_F^2 + \lambda Q(\boldsymbol{W}).$$

- Both (P2.1.1) and (P2.1.2) have closed form solutions.

GTLMRI: Denoising

- Two alternating steps for (P2.2) become as follows.

$$\text{(P2.2.1)} \min_{\mathcal{A}} \|\boldsymbol{W}\hat{\mathcal{X}} - \mathcal{A}\|_F^2 + \beta\|\mathcal{A}\|_1.$$

$$\text{(P2.2.2)} \min_{\hat{\mathcal{X}}} \|\boldsymbol{W}\hat{\mathcal{X}} - \mathcal{A}\|_F^2 + \tau\|\mathcal{R}(\boldsymbol{x}) - \hat{\mathcal{X}}\|_F^2.$$

- (P2.2.1) is again solved by soft thresholding.
- (P2.2.2) has a simple least squares solution for fixed $\mathcal{A}$ given by $(\boldsymbol{W}^H\boldsymbol{W} + \tau\boldsymbol{I})^{-1}(\boldsymbol{W}^H\mathcal{A} + \tau\mathcal{R}(\boldsymbol{x}))$.

GTLMRI: Denoising

- Two alternating steps for (P2.2) become as follows.

$$\text{(P2.2.1)} \min_{\mathcal{A}} \|\boldsymbol{W}\hat{\mathcal{X}} - \mathcal{A}\|_F^2 + \beta\|\mathcal{A}\|_1.$$

$$\text{(P2.2.2)} \min_{\hat{\mathcal{X}}} \|\boldsymbol{W}\hat{\mathcal{X}} - \mathcal{A}\|_F^2 + \tau\|\mathcal{R}(\boldsymbol{x}) - \hat{\mathcal{X}}\|_F^2.$$

- (P2.2.1) is again solved by soft thresholding.
- (P2.2.2) has a simple least squares solution for fixed $\mathcal{A}$ given by $(\boldsymbol{W}^H\boldsymbol{W} + \tau\boldsymbol{I})^{-1}(\boldsymbol{W}^H\mathcal{A} + \tau\mathcal{R}(\boldsymbol{x}))$.

GTLMRI: Denoising

- Two alternating steps for (P2.2) become as follows.

$$\text{(P2.2.1)} \min_{\boldsymbol{\mathcal{A}}} \|\boldsymbol{W}\hat{\boldsymbol{\mathcal{X}}} - \boldsymbol{\mathcal{A}}\|_F^2 + \beta\|\boldsymbol{\mathcal{A}}\|_1.$$

$$\text{(P2.2.2)} \min_{\hat{\boldsymbol{\mathcal{X}}}} \|\boldsymbol{W}\hat{\boldsymbol{\mathcal{X}}} - \boldsymbol{\mathcal{A}}\|_F^2 + \tau\|\mathcal{R}(\boldsymbol{x}) - \hat{\boldsymbol{\mathcal{X}}}\|_F^2.$$

- (P2.2.1) is again solved by soft thresholding.
- (P2.2.2) has a simple least squares solution for fixed $\boldsymbol{\mathcal{A}}$ given by $(\boldsymbol{W}^H\boldsymbol{W} + \tau\boldsymbol{I})^{-1}(\boldsymbol{W}^H\boldsymbol{\mathcal{A}} + \tau\mathcal{R}(\boldsymbol{x}))$.

GTLMRI: Denoising

- Two alternating steps for (P2.2) become as follows.

$$\text{(P2.2.1)} \min_{\boldsymbol{\mathcal{A}}} \|\boldsymbol{W}\hat{\boldsymbol{\mathcal{X}}} - \boldsymbol{\mathcal{A}}\|_F^2 + \beta\|\boldsymbol{\mathcal{A}}\|_1.$$

$$\text{(P2.2.2)} \min_{\hat{\boldsymbol{\mathcal{X}}}} \|\boldsymbol{W}\hat{\boldsymbol{\mathcal{X}}} - \boldsymbol{\mathcal{A}}\|_F^2 + \tau\|\boldsymbol{\mathcal{R}}(\boldsymbol{x}) - \hat{\boldsymbol{\mathcal{X}}}\|_F^2.$$

- (P2.2.1) is again solved by soft thresholding.
- (P2.2.2) has a simple least squares solution for fixed $\boldsymbol{\mathcal{A}}$ given by $(\boldsymbol{W}^H\boldsymbol{W} + \tau\boldsymbol{I})^{-1}(\boldsymbol{W}^H\boldsymbol{\mathcal{A}} + \tau\boldsymbol{\mathcal{R}}(\boldsymbol{x}))$.

GTLMRI: Denoising

- Two alternating steps for (P2.2) become as follows.

$$\text{(P2.2.1)} \min_{\boldsymbol{\mathcal{A}}} \|\boldsymbol{W}\hat{\boldsymbol{\mathcal{X}}} - \boldsymbol{\mathcal{A}}\|_F^2 + \beta\|\boldsymbol{\mathcal{A}}\|_1.$$

$$\text{(P2.2.2)} \min_{\hat{\boldsymbol{\mathcal{X}}}} \|\boldsymbol{W}\hat{\boldsymbol{\mathcal{X}}} - \boldsymbol{\mathcal{A}}\|_F^2 + \tau\|\boldsymbol{\mathcal{R}}(\boldsymbol{x}) - \hat{\boldsymbol{\mathcal{X}}}\|_F^2.$$

- (P2.2.1) is again solved by soft thresholding.
- (P2.2.2) has a simple least squares solution for fixed $\mathcal{A}$ given by $(\boldsymbol{W}^H\boldsymbol{W} + \tau\boldsymbol{I})^{-1}(\boldsymbol{W}^H\mathcal{A} + \tau\mathcal{R}(\boldsymbol{x}))$.

GTLMRI: Denoising

- Two alternating steps for (P2.2) become as follows.

$$\text{(P2.2.1)} \min_{\boldsymbol{\mathcal{A}}} \|\boldsymbol{W}\hat{\boldsymbol{\mathcal{X}}} - \boldsymbol{\mathcal{A}}\|_F^2 + \beta\|\boldsymbol{\mathcal{A}}\|_1.$$

$$\text{(P2.2.2)} \min_{\hat{\boldsymbol{\mathcal{X}}}} \|\boldsymbol{W}\hat{\boldsymbol{\mathcal{X}}} - \boldsymbol{\mathcal{A}}\|_F^2 + \tau\|\mathcal{R}(\boldsymbol{x}) - \hat{\boldsymbol{\mathcal{X}}}\|_F^2.$$

- (P2.2.1) is again solved by soft thresholding.
- (P2.2.2) has a simple least squares solution for fixed $\boldsymbol{\mathcal{A}}$ given by $(\boldsymbol{W}^H\boldsymbol{W} + \tau\boldsymbol{I})^{-1}(\boldsymbol{W}^H\boldsymbol{\mathcal{A}} + \tau\mathcal{R}(\boldsymbol{x}))$.

Outline

1 Introduction
- The Problem
- The Novel Approach

2 Transform Learning MRI

3 GTLMRI
- New Cost
- GTLMRI: Denoising
- GTLMRI: Reconstruction
- GTLMRI: Overall Algorithm

4 Simulations and Conclusion

GTLMRI: Reconstruction

- The second main step for the solution of (P1) is the reconstruction step, (P3).

$$(\text{P3}) \min_{\boldsymbol{x}} \frac{1}{2}\|\mathcal{F}_u \boldsymbol{x} - \boldsymbol{y}\|_2^2 + \frac{\tau}{2\eta}\|\mathcal{R}(\boldsymbol{x}) - \hat{\mathcal{X}}\|_F^2 + \frac{\upsilon'}{2\eta}\|\boldsymbol{\Phi x}\|_1.$$

GTLMRI: Reconstruction

- The second main step for the solution of (P1) is the reconstruction step, (P3).

$$(\mathrm{P3})\ \min_{\boldsymbol{x}} \frac{1}{2}\|\mathcal{F}_u \boldsymbol{x} - \boldsymbol{y}\|_2^2 + \frac{\tau}{2\eta}\|\mathcal{R}(\boldsymbol{x}) - \hat{\mathcal{X}}\|_F^2 + \frac{\upsilon'}{2\eta}\|\boldsymbol{\Phi}\boldsymbol{x}\|_1.$$

GTLMRI: Reconstruction

- The second main step for the solution of (P1) is the reconstruction step, (P3).

$$\text{(P3)} \min_{\boldsymbol{x}} \frac{1}{2}\|\mathcal{F}_u \boldsymbol{x} - \boldsymbol{y}\|_2^2 + \frac{\tau}{2\eta}\|\mathcal{R}(\boldsymbol{x}) - \hat{\boldsymbol{\mathcal{X}}}\|_F^2 + \frac{\upsilon'}{2\eta}\|\boldsymbol{\Phi}\boldsymbol{x}\|_1.$$

GTLMRI: Reconstruction

- Define patch to image operator $\hat{\mathcal{R}}$.
- $\hat{\mathcal{R}}(\hat{\mathcal{X}}) = (\sum_j \boldsymbol{R}_j^T \hat{\mathbf{x}}_j)./\boldsymbol{w}$.
- (P3) can be approximately rewritten as follows.

$$(\text{P3}')\ \min_{\boldsymbol{x}} \tfrac{1}{2}(\|\mathcal{F}_u\boldsymbol{x} - \boldsymbol{y}\|_2^2 + \tau'\|\boldsymbol{x} - \hat{\mathcal{R}}(\hat{\mathcal{X}})\|_2^2) + \upsilon\|\boldsymbol{\Phi}\boldsymbol{x}\|_1. \quad (6)$$

$$(\text{P3})\ \min_{\boldsymbol{x}} \tfrac{1}{2}\|\mathcal{F}_u\boldsymbol{x} - \boldsymbol{y}\|_2^2 + \tfrac{\tau}{2\eta}\|\mathcal{R}(\boldsymbol{x}) - \hat{\mathcal{X}}\|_F^2 + \tfrac{\upsilon'}{2\eta}\|\boldsymbol{\Phi}\boldsymbol{x}\|_1.$$

GTLMRI: Reconstruction

- Define patch to image operator $\hat{\mathcal{R}}$.
- $\hat{\mathcal{R}}(\hat{\mathcal{X}}) = (\sum_j \boldsymbol{R}_j^T \hat{\boldsymbol{x}}_j)./\boldsymbol{w}$.
- (P3) can be approximately rewritten as follows.

$$\text{(P3}') \min_{\boldsymbol{x}} \frac{1}{2}(\|\mathcal{F}_u \boldsymbol{x} - \boldsymbol{y}\|_2^2 + \tau' \|\boldsymbol{x} - \hat{\mathcal{R}}(\hat{\mathcal{X}})\|_2^2) + \upsilon \|\boldsymbol{\Phi x}\|_1. \quad (6)$$

$$\text{(P3)} \min_{\boldsymbol{x}} \frac{1}{2}\|\mathcal{F}_u \boldsymbol{x} - \boldsymbol{y}\|_2^2 + \frac{\tau}{2\eta}\|\mathcal{R}(\boldsymbol{x}) - \hat{\mathcal{X}}\|_F^2 + \frac{\upsilon'}{2\eta}\|\boldsymbol{\Phi x}\|_1.$$

GTLMRI: Reconstruction

- Define patch to image operator $\hat{\mathcal{R}}$.
- $\hat{\mathcal{R}}(\hat{\mathcal{X}}) = (\sum_j \boldsymbol{R}_j^T \hat{\boldsymbol{x}}_j)./\boldsymbol{w}$.
- (P3) can be approximately rewritten as follows.

$$(\text{P3}')\ \min_{\boldsymbol{x}} \frac{1}{2}(\|\mathcal{F}_u\boldsymbol{x} - \boldsymbol{y}\|_2^2 + \tau'\|\boldsymbol{x} - \hat{\mathcal{R}}(\hat{\mathcal{X}})\|_2^2) + \upsilon\|\boldsymbol{\Phi x}\|_1. \quad (6)$$

$$(\text{P3})\ \min_{\boldsymbol{x}} \frac{1}{2}\|\mathcal{F}_u\boldsymbol{x} - \boldsymbol{y}\|_2^2 + \frac{\tau}{2\eta}\|\mathcal{R}(\boldsymbol{x}) - \hat{\mathcal{X}}\|_F^2 + \frac{\upsilon'}{2\eta}\|\boldsymbol{\Phi x}\|_1.$$

GTLMRI: Reconstruction

- Define patch to image operator $\hat{\mathcal{R}}$.
- $\hat{\mathcal{R}}(\hat{\mathcal{X}}) = (\sum_j \boldsymbol{R}_j^T \hat{\boldsymbol{x}}_j)./\boldsymbol{w}$.
- (P3) can be approximately rewritten as follows.

$$\text{(P3}'\text{)} \min_{\boldsymbol{x}} \frac{1}{2}(\|\mathcal{F}_u \boldsymbol{x} - \boldsymbol{y}\|_2^2 + \tau' \|\boldsymbol{x} - \hat{\mathcal{R}}(\hat{\mathcal{X}})\|_2^2) + \upsilon \|\boldsymbol{\Phi x}\|_1. \quad (6)$$

$$\text{(P3)} \min_{\boldsymbol{x}} \frac{1}{2}\|\mathcal{F}_u \boldsymbol{x} - \boldsymbol{y}\|_2^2 + \frac{\tau}{2\eta}\|\mathcal{R}(\boldsymbol{x}) - \hat{\mathcal{X}}\|_F^2 + \frac{\upsilon'}{2\eta}\|\boldsymbol{\Phi x}\|_1.$$

GTLMRI: Reconstruction

- Define patch to image operator $\hat{\mathcal{R}}$.
- $\hat{\mathcal{R}}(\hat{\mathcal{X}}) = \left(\sum_j \boldsymbol{R}_j^T \hat{\boldsymbol{x}}_j\right)./\boldsymbol{w}$.
- (P3) can be approximately rewritten as follows.

$$\text{(P3}'\text{)} \min_{\boldsymbol{x}} \frac{1}{2}\left(\|\mathcal{F}_u \boldsymbol{x} - \boldsymbol{y}\|_2^2 + \tau' \|\boldsymbol{x} - \hat{\mathcal{R}}(\hat{\mathcal{X}})\|_2^2\right) + \upsilon \|\boldsymbol{\Phi x}\|_1. \quad (6)$$

$$\text{(P3)} \min_{\boldsymbol{x}} \frac{1}{2}\|\mathcal{F}_u \boldsymbol{x} - \boldsymbol{y}\|_2^2 + \frac{\tau}{2\eta}\|\mathcal{R}(\boldsymbol{x}) - \hat{\mathcal{X}}\|_F^2 + \frac{\upsilon'}{2\eta}\|\boldsymbol{\Phi x}\|_1.$$

GTLMRI: Reconstruction

- Define patch to image operator $\hat{\mathcal{R}}$.
- $\hat{\mathcal{R}}(\hat{\mathcal{X}}) = (\sum_j \boldsymbol{R}_j^T \hat{\boldsymbol{x}}_j)./\boldsymbol{w}$.
- (P3) can be approximately rewritten as follows.

$$(\text{P3}') \min_{\boldsymbol{x}} \frac{1}{2}\left(\|\mathcal{F}_u\boldsymbol{x} - \boldsymbol{y}\|_2^2 + \tau'\|\boldsymbol{x} - \hat{\mathcal{R}}(\hat{\mathcal{X}})\|_2^2\right) + \upsilon\|\boldsymbol{\Phi x}\|_1. \quad (6)$$

$$(\text{P3}) \min_{\boldsymbol{x}} \frac{1}{2}\|\mathcal{F}_u\boldsymbol{x} - \boldsymbol{y}\|_2^2 + \frac{\tau}{2\eta}\|\mathcal{R}(\boldsymbol{x}) - \hat{\mathcal{X}}\|_F^2 + \frac{\upsilon'}{2\eta}\|\boldsymbol{\Phi x}\|_1.$$

GTLMRI: Reconstruction

- Define two functions:
- $g(\boldsymbol{x}) = \frac{1}{2}(\|\mathcal{F}_u\boldsymbol{x} - \boldsymbol{y}\|_2^2 + \tau'\|\boldsymbol{x} - \hat{\mathcal{R}}(\hat{\mathcal{X}})\|_2^2)$
- $f(\boldsymbol{x}) = \upsilon\|\boldsymbol{\Phi x}\|_1$.

$$(\text{P3}')\ \min_{\boldsymbol{x}} f(\boldsymbol{x}) + g(\boldsymbol{x}).$$

- This problem can be solved very efficiently by proximal splitting methods.
- We have used the forward-backward splitting algorithm.

GTLMRI: Reconstruction

- Define two functions:
- $g(\boldsymbol{x}) = \frac{1}{2}(\|\mathcal{F}_u\boldsymbol{x} - \boldsymbol{y}\|_2^2 + \tau'\|\boldsymbol{x} - \hat{\mathcal{R}}(\hat{\mathcal{X}})\|_2^2)$
- $f(\boldsymbol{x}) = \upsilon\|\boldsymbol{\Phi x}\|_1$.

$$(\mathrm{P3}') \min_{\boldsymbol{x}} f(\boldsymbol{x}) + g(\boldsymbol{x}).$$

- This problem can be solved very efficiently by proximal splitting methods.
- We have used the forward-backward splitting algorithm.

GTLMRI: Reconstruction

- Define two functions:
- $g(\boldsymbol{x}) = \frac{1}{2}(\|\mathcal{F}_u\boldsymbol{x} - \boldsymbol{y}\|_2^2 + \tau'\|\boldsymbol{x} - \hat{\mathcal{R}}(\hat{\mathcal{X}})\|_2^2)$
- $f(\boldsymbol{x}) = \upsilon\|\boldsymbol{\Phi x}\|_1$.

$$(\mathrm{P3}')\ \min_{\boldsymbol{x}} f(\boldsymbol{x}) + g(\boldsymbol{x}).$$

- This problem can be solved very efficiently by proximal splitting methods.
- We have used the forward-backward splitting algorithm.

GTLMRI: Reconstruction

- Define two functions:
- $g(\boldsymbol{x}) = \frac{1}{2}(\|\mathcal{F}_u\boldsymbol{x} - \boldsymbol{y}\|_2^2 + \tau'\|\boldsymbol{x} - \hat{\mathcal{R}}(\hat{\mathcal{X}})\|_2^2)$
- $f(\boldsymbol{x}) = \upsilon\|\boldsymbol{\Phi}\boldsymbol{x}\|_1$.

$$(\mathrm{P3}')\ \min_{\boldsymbol{x}} f(\boldsymbol{x}) + g(\boldsymbol{x}).$$

- This problem can be solved very efficiently by proximal splitting methods.
- We have used the forward-backward splitting algorithm.

GTLMRI: Reconstruction

- Define two functions:
- $g(\boldsymbol{x}) = \frac{1}{2}\left(\|\mathcal{F}_u \boldsymbol{x} - \boldsymbol{y}\|_2^2 + \tau' \|\boldsymbol{x} - \hat{\mathcal{R}}(\hat{\mathcal{X}})\|_2^2\right)$
- $f(\boldsymbol{x}) = \upsilon \|\boldsymbol{\Phi x}\|_1$.

$$(\text{P3}') \min_{\boldsymbol{x}} f(\boldsymbol{x}) + g(\boldsymbol{x}).$$

- This problem can be solved very efficiently by proximal splitting methods.
- We have used the forward-backward splitting algorithm.

GTLMRI: Reconstruction

- Define two functions:
- $g(\boldsymbol{x}) = \frac{1}{2}(\|\mathcal{F}_u\boldsymbol{x} - \boldsymbol{y}\|_2^2 + \tau'\|\boldsymbol{x} - \hat{\mathcal{R}}(\hat{\mathcal{X}})\|_2^2)$
- $f(\boldsymbol{x}) = \upsilon\|\boldsymbol{\Phi x}\|_1$.

$$(\text{P3}')\ \min_{\boldsymbol{x}} f(\boldsymbol{x}) + g(\boldsymbol{x}).$$

- This problem can be solved very efficiently by proximal splitting methods.
- We have used the forward-backward splitting algorithm.

GTLMRI: Reconstruction

- Define two functions:
- $g(\boldsymbol{x}) = \frac{1}{2}(\|\mathcal{F}_u \boldsymbol{x} - \boldsymbol{y}\|_2^2 + \tau' \|\boldsymbol{x} - \hat{\mathcal{R}}(\hat{\mathcal{X}})\|_2^2)$
- $f(\boldsymbol{x}) = \upsilon \|\boldsymbol{\Phi x}\|_1$.

$$(\text{P3}') \min_{\boldsymbol{x}} f(\boldsymbol{x}) + g(\boldsymbol{x}).$$

- This problem can be solved very efficiently by proximal splitting methods.
- We have used the forward-backward splitting algorithm.

GTLMRI: Reconstruction

- The forward-backward splitting steps:

$$\text{(P3.1)} \quad \boldsymbol{z} = \boldsymbol{x} - \gamma \nabla g(\boldsymbol{x}). \tag{7}$$

$$\text{(P3.2)} \quad \boldsymbol{x} = \boldsymbol{x} + \mu(\text{prox}_{\gamma f}(\boldsymbol{z}) - \boldsymbol{x}). \tag{8}$$

- $\nabla g(\boldsymbol{x}) = \mathcal{F}_u^H(\mathcal{F}_u \boldsymbol{x} - \boldsymbol{y}) + \tau'(\boldsymbol{x} - \hat{\mathcal{R}}(\hat{\mathcal{X}}))$.
- $\mathcal{F}_u^H$ is the adjoint operator of $\mathcal{F}_u$, it realizes zero-filled reconstruction.
- $\text{prox}_{\gamma f}(\cdot)$ is realized by soft thresholding in the transform (Φ) domain and taking an inverse transform.

GTLMRI: Reconstruction

- The forward-backward splitting steps:

$$\text{(P3.1)} \quad \boldsymbol{z} = \boldsymbol{x} - \gamma \nabla g(\boldsymbol{x}). \tag{7}$$

$$\text{(P3.2)} \quad \boldsymbol{x} = \boldsymbol{x} + \mu(\text{prox}_{\gamma f}(\boldsymbol{z}) - \boldsymbol{x}). \tag{8}$$

- $\nabla g(\boldsymbol{x}) = \mathcal{F}_u^H(\mathcal{F}_u \boldsymbol{x} - \boldsymbol{y}) + \tau'(\boldsymbol{x} - \hat{\mathcal{R}}(\hat{\mathcal{X}}))$.
- $\mathcal{F}_u^H$ is the adjoint operator of $\mathcal{F}_u$, it realizes zero-filled reconstruction.
- $\text{prox}_{\gamma f}(\cdot)$ is realized by soft thresholding in the transform (Φ) domain and taking an inverse transform.

GTLMRI: Reconstruction

- The forward-backward splitting steps:

$$\text{(P3.1)} \quad \boldsymbol{z} = \boldsymbol{x} - \gamma \nabla g(\boldsymbol{x}). \tag{7}$$

$$\text{(P3.2)} \quad \boldsymbol{x} = \boldsymbol{x} + \mu(\mathrm{prox}_{\gamma f}(\boldsymbol{z}) - \boldsymbol{x}). \tag{8}$$

- $\nabla g(\boldsymbol{x}) = \mathcal{F}_u^H(\mathcal{F}_u \boldsymbol{x} - \boldsymbol{y}) + \tau'(\boldsymbol{x} - \hat{\mathcal{R}}(\hat{\mathcal{X}}))$.
- $\mathcal{F}_u^H$ is the adjoint operator of $\mathcal{F}_u$, it realizes zero-filled reconstruction.
- $\mathrm{prox}_{\gamma f}(\cdot)$ is realized by soft thresholding in the transform (Φ) domain and taking an inverse transform.

GTLMRI: Reconstruction

- The forward-backward splitting steps:

$$\text{(P3.1)} \quad \boldsymbol{z} = \boldsymbol{x} - \gamma \nabla g(\boldsymbol{x}). \tag{7}$$

$$\text{(P3.2)} \quad \boldsymbol{x} = \boldsymbol{x} + \mu(\text{prox}_{\gamma f}(\boldsymbol{z}) - \boldsymbol{x}). \tag{8}$$

- $\nabla g(\boldsymbol{x}) = \mathcal{F}_u^H(\mathcal{F}_u \boldsymbol{x} - \boldsymbol{y}) + \tau'(\boldsymbol{x} - \hat{\mathcal{R}}(\hat{\mathcal{X}}))$.
- $\mathcal{F}_u^H$ is the adjoint operator of $\mathcal{F}_u$, it realizes zero-filled reconstruction.
- $\text{prox}_{\gamma f}(\cdot)$ is realized by soft thresholding in the transform $(\boldsymbol{\Phi})$ domain and taking an inverse transform.

GTLMRI: Reconstruction

- The forward-backward splitting steps:

$$\text{(P3.1)} \quad \boldsymbol{z} = \boldsymbol{x} - \gamma \nabla g(\boldsymbol{x}). \tag{7}$$

$$\text{(P3.2)} \quad \boldsymbol{x} = \boldsymbol{x} + \mu(\text{prox}_{\gamma f}(\boldsymbol{z}) - \boldsymbol{x}). \tag{8}$$

- $\nabla g(\boldsymbol{x}) = \mathcal{F}_u^H(\mathcal{F}_u \boldsymbol{x} - \boldsymbol{y}) + \tau'(\boldsymbol{x} - \hat{\mathcal{R}}(\hat{\mathcal{X}}))$.
- $\mathcal{F}_u^H$ is the adjoint operator of $\mathcal{F}_u$, it realizes zero-filled reconstruction.
- $\text{prox}_{\gamma f}(\cdot)$ is realized by soft thresholding in the transform ($\boldsymbol{\Phi}$) domain and taking an inverse transform.

GTLMRI: Reconstruction

- The forward-backward splitting steps:

$$\text{(P3.1)} \quad \boldsymbol{z} = \boldsymbol{x} - \gamma \nabla g(\boldsymbol{x}). \tag{7}$$

$$\text{(P3.2)} \quad \boldsymbol{x} = \boldsymbol{x} + \mu(\text{prox}_{\gamma f}(\boldsymbol{z}) - \boldsymbol{x}). \tag{8}$$

- $\nabla g(\boldsymbol{x}) = \mathcal{F}_u^H(\mathcal{F}_u \boldsymbol{x} - \boldsymbol{y}) + \tau'(\boldsymbol{x} - \hat{\mathcal{R}}(\hat{\mathcal{X}}))$.
- $\mathcal{F}_u^H$ is the adjoint operator of $\mathcal{F}_u$, it realizes zero-filled reconstruction.
- $\text{prox}_{\gamma f}(\cdot)$ is realized by soft thresholding in the transform ($\boldsymbol{\Phi}$) domain and taking an inverse transform.

GTLMRI: Reconstruction

- The forward-backward splitting steps:

$$\text{(P3.1)} \quad \boldsymbol{z} = \boldsymbol{x} - \gamma \nabla g(\boldsymbol{x}). \tag{7}$$

$$\text{(P3.2)} \quad \boldsymbol{x} = \boldsymbol{x} + \mu(\mathrm{prox}_{\gamma f}(\boldsymbol{z}) - \boldsymbol{x}). \tag{8}$$

- $\nabla g(\boldsymbol{x}) = \mathcal{F}_u^H(\mathcal{F}_u \boldsymbol{x} - \boldsymbol{y}) + \tau'(\boldsymbol{x} - \hat{\mathcal{R}}(\hat{\mathcal{X}}))$.
- $\mathcal{F}_u^H$ is the adjoint operator of $\mathcal{F}_u$, it realizes zero-filled reconstruction.
- $\mathrm{prox}_{\gamma f}(\cdot)$ is realized by soft thresholding in the transform ($\boldsymbol{\Phi}$) domain and taking an inverse transform.

Outline

1. Introduction
   - The Problem
   - The Novel Approach
2. Transform Learning MRI
3. GTLMRI
   - New Cost
   - GTLMRI: Denoising
   - GTLMRI: Reconstruction
   - GTLMRI: Overall Algorithm
4. Simulations and Conclusion

GTLMRI: Overall Algorithm

- *Input*: Observation, $\boldsymbol{y} = \mathcal{F}_u \boldsymbol{x}^\star + \eta$; parameters $\lambda, \beta, \tau, \tau', \upsilon, \gamma, \mu$.
- *Goal*:
$$\min_{\boldsymbol{W}, \hat{\mathcal{X}}, \mathcal{A}, \boldsymbol{x}} \|\boldsymbol{W}\hat{\mathcal{X}} - \mathcal{A}\|_F^2 + \lambda Q(\boldsymbol{W}) + \beta\|\mathcal{A}\|_1 + \tau\|\mathcal{R}(\boldsymbol{x}) - \hat{\mathcal{X}}\|_F^2 + \eta\|\mathcal{F}_u \boldsymbol{x} - \boldsymbol{y}\|_2^2 + \upsilon'\|\boldsymbol{\Phi x}\|_1$$

- Initialize $\boldsymbol{x} = \mathcal{F}_u^H \boldsymbol{y}$.
- Main iteration:
  - Initialize $\hat{\mathcal{X}} = \mathcal{R}(\boldsymbol{x})$. *denoising stage*
  - Iterate (P2.1), N_1 times.
  - Iterate (P2.2), N_2 times.
  - Initialize $\boldsymbol{x} = \mathcal{R}(\hat{\mathcal{X}})$. *reconstruction stage*
  - Iterate (P3.1-P3.2), N_3 times.
- Output reconstructed MR image $\boldsymbol{x}$.

GTLMRI: Overall Algorithm

- *Input*: Observation, $\boldsymbol{y} = \mathcal{F}_u \boldsymbol{x}^\star + \eta$; parameters $\lambda, \beta, \tau, \tau', \upsilon, \gamma, \mu$.
- *Goal*: $\min_{\boldsymbol{W}, \hat{\mathcal{X}}, \mathcal{A}, \boldsymbol{x}} \|\boldsymbol{W}\hat{\mathcal{X}} - \mathcal{A}\|_F^2 + \lambda Q(\boldsymbol{W}) + \beta\|\mathcal{A}\|_1$

$$+\tau\|\mathcal{R}(\boldsymbol{x}) - \hat{\mathcal{X}}\|_F^2 + \eta\|\mathcal{F}_u \boldsymbol{x} - \boldsymbol{y}\|_2^2 + \upsilon'\|\boldsymbol{\Phi x}\|_1$$

- Initialize $\boldsymbol{x} = \mathcal{F}_u^H \boldsymbol{y}$.
- Main iteration:
  - Initialize $\hat{\mathcal{X}} = \mathcal{R}(\boldsymbol{x})$. *denoising starts*
  - Iterate (P2.1), N_1 times.
  - Iterate (P2.2), N_2 times.
  - Initialize $\boldsymbol{x} = \hat{\mathcal{R}}(\hat{\mathcal{X}})$. *reconstruction starts*
  - Iterate (P3.1-P3.2), N_3 times.
- Output reconstructed MR image $\boldsymbol{x}$.

GTLMRI: Overall Algorithm

- *Input*: Observation, $\boldsymbol{y} = \mathcal{F}_u \boldsymbol{x}^\star + \boldsymbol{\eta}$; parameters $\lambda, \beta, \tau, \tau', \upsilon, \gamma, \mu$.
- *Goal*: $$\min_{\boldsymbol{W}, \hat{\mathcal{X}}, \mathcal{A}, \boldsymbol{x}} \|\boldsymbol{W}\hat{\mathcal{X}} - \mathcal{A}\|_F^2 + \lambda Q(\boldsymbol{W}) + \beta\|\mathcal{A}\|_1 + \tau\|\mathcal{R}(\boldsymbol{x}) - \hat{\mathcal{X}}\|_F^2 + \eta\|\mathcal{F}_u\boldsymbol{x} - \boldsymbol{y}\|_2^2 + \upsilon'\|\boldsymbol{\Phi x}\|_1$$

- Initialize $\boldsymbol{x} = \mathcal{F}_u^H \boldsymbol{y}$.
- Main iteration:
  - Initialize $\hat{\mathcal{X}} = \mathcal{R}(\boldsymbol{x})$. *denoising starts*
  - Iterate (P2.1), N_1 times.
  - Iterate (P2.2), N_2 times.
  - Initialize $\boldsymbol{x} = \hat{\mathcal{R}}(\hat{\mathcal{X}})$. *reconstruction starts*
  - Iterate (P3.1-P3.2), N_3 times.
- Output reconstructed MR image $\boldsymbol{x}$.

GTLMRI: Overall Algorithm

- *Input*: Observation, $\boldsymbol{y} = \mathcal{F}_u \boldsymbol{x}^\star + \eta$; parameters $\lambda, \beta, \tau, \tau', \upsilon, \gamma, \mu$.
- *Goal*: $$\min_{\boldsymbol{W}, \hat{\mathcal{X}}, \mathcal{A}, \boldsymbol{x}} \|\boldsymbol{W}\hat{\mathcal{X}} - \mathcal{A}\|_F^2 + \lambda Q(\boldsymbol{W}) + \beta\|\mathcal{A}\|_1 + \tau\|\mathcal{R}(\boldsymbol{x}) - \hat{\mathcal{X}}\|_F^2 + \eta\|\mathcal{F}_u\boldsymbol{x} - \boldsymbol{y}\|_2^2 + \upsilon'\|\boldsymbol{\Phi}\boldsymbol{x}\|_1$$

- Initialize $\boldsymbol{x} = \mathcal{F}_u^H \boldsymbol{y}$.
- Main iteration:
  - Initialize $\hat{\mathcal{X}} = \mathcal{R}(\boldsymbol{x})$. *denoising starts*
  - Iterate (P2.1), N_1 times.
  - Iterate (P2.2), N_2 times.
  - Initialize $\boldsymbol{x} = \hat{\mathcal{R}}(\hat{\mathcal{X}})$. *reconstruction starts*
  - Iterate (P3.1-P3.2), N_3 times.
- Output reconstructed MR image $\boldsymbol{x}$.

GTLMRI: Overall Algorithm

- *Input*: Observation, $\boldsymbol{y} = \mathcal{F}_u \boldsymbol{x}^\star + \boldsymbol{\eta}$; parameters $\lambda, \beta, \tau, \tau', \upsilon, \gamma, \mu$.
- *Goal*: $\min_{\boldsymbol{W}, \hat{\mathcal{X}}, \mathcal{A}, \boldsymbol{x}} \|\boldsymbol{W}\hat{\mathcal{X}} - \mathcal{A}\|_F^2 + \lambda Q(\boldsymbol{W}) + \beta\|\mathcal{A}\|_1$
  $+\tau\|\mathcal{R}(\boldsymbol{x}) - \hat{\mathcal{X}}\|_F^2 + \eta\|\mathcal{F}_u\boldsymbol{x} - \boldsymbol{y}\|_2^2 + \upsilon'\|\boldsymbol{\Phi}\boldsymbol{x}\|_1$

- Initialize $\boldsymbol{x} = \mathcal{F}_u^H \boldsymbol{y}$.
- Main iteration:
  - Initialize $\hat{\mathcal{X}} = \mathcal{R}(\boldsymbol{x})$. *denoising starts*
  - Iterate (P2.1), N_1 times.
  - Iterate (P2.2), N_2 times.
  - Initialize $\boldsymbol{x} = \hat{\mathcal{R}}(\hat{\mathcal{X}})$. *reconstruction starts*
  - Iterate (P3.1-P3.2), N_3 times.
- Output reconstructed MR image $\boldsymbol{x}$.

GTLMRI: Overall Algorithm

- *Input*: Observation, $\boldsymbol{y} = \mathcal{F}_u \boldsymbol{x}^\star + \eta$; parameters $\lambda, \beta, \tau, \tau', \upsilon, \gamma, \mu$.
- *Goal*: $\min\limits_{\boldsymbol{W}, \hat{\mathcal{X}}, \mathcal{A}, \boldsymbol{x}} \|\boldsymbol{W}\hat{\mathcal{X}} - \mathcal{A}\|_F^2 + \lambda Q(\boldsymbol{W}) + \beta\|\mathcal{A}\|_1$

$$+\tau\|\mathcal{R}(\boldsymbol{x}) - \hat{\mathcal{X}}\|_F^2 + \eta\|\mathcal{F}_u\boldsymbol{x} - \boldsymbol{y}\|_2^2 + \upsilon'\|\boldsymbol{\Phi x}\|_1$$

- Initialize $\boldsymbol{x} = \mathcal{F}_u^H \boldsymbol{y}$.
- Main iteration:
  - Initialize $\hat{\mathcal{X}} = \mathcal{R}(\boldsymbol{x})$. *denoising starts*
  - Iterate (P2.1), N_1 times.
  - Iterate (P2.2), N_2 times.
  - Initialize $\boldsymbol{x} = \hat{\mathcal{R}}(\hat{\mathcal{X}})$. *reconstruction starts*
  - Iterate (P3.1-P3.2), N_3 times.
- Output reconstructed MR image $\boldsymbol{x}$.

GTLMRI: Overall Algorithm

- *Input*: Observation, $\boldsymbol{y} = \mathcal{F}_u \boldsymbol{x}^\star + \eta$; parameters $\lambda, \beta, \tau, \tau', \upsilon, \gamma, \mu$.
- *Goal*: $\min_{\boldsymbol{W}, \hat{\mathcal{X}}, \mathcal{A}, \boldsymbol{x}} \|\boldsymbol{W}\hat{\mathcal{X}} - \mathcal{A}\|_F^2 + \lambda Q(\boldsymbol{W}) + \beta \|\mathcal{A}\|_1$

$$+\tau \|\mathcal{R}(\boldsymbol{x}) - \hat{\mathcal{X}}\|_F^2 + \eta \|\mathcal{F}_u \boldsymbol{x} - \boldsymbol{y}\|_2^2 + \upsilon' \|\boldsymbol{\Phi x}\|_1$$

- Initialize $\boldsymbol{x} = \mathcal{F}_u^H \boldsymbol{y}$.
- Main iteration:
  - Initialize $\hat{\mathcal{X}} = \mathcal{R}(\boldsymbol{x})$. *denoising starts*
  - Iterate (P2.1), N_1 times.
  - Iterate (P2.2), N_2 times.
  - Initialize $\boldsymbol{x} = \hat{\mathcal{R}}(\hat{\mathcal{X}})$. *reconstruction starts*
  - Iterate (P3.1-P3.2), N_3 times.
- Output reconstructed MR image $\boldsymbol{x}$.

GTLMRI: Overall Algorithm

- *Input*: Observation, $\boldsymbol{y} = \mathcal{F}_u \boldsymbol{x}^\star + \eta$; parameters $\lambda, \beta, \tau, \tau', \upsilon, \gamma, \mu$.
- *Goal*: $\min_{\boldsymbol{W}, \hat{\mathcal{X}}, \mathcal{A}, \boldsymbol{x}} \|\boldsymbol{W}\hat{\mathcal{X}} - \mathcal{A}\|_F^2 + \lambda Q(\boldsymbol{W}) + \beta\|\mathcal{A}\|_1$
  $+\tau\|\mathcal{R}(\boldsymbol{x}) - \hat{\mathcal{X}}\|_F^2 + \eta\|\mathcal{F}_u\boldsymbol{x} - \boldsymbol{y}\|_2^2 + \upsilon'\|\boldsymbol{\Phi x}\|_1$

- Initialize $\boldsymbol{x} = \mathcal{F}_u^H \boldsymbol{y}$.
- Main iteration:
  - Initialize $\hat{\mathcal{X}} = \mathcal{R}(\boldsymbol{x})$. *denoising starts*
  - Iterate (P2.1), N_1 times.
  - Iterate (P2.2), N_2 times.
  - Initialize $\boldsymbol{x} = \hat{\mathcal{R}}(\hat{\mathcal{X}})$. *reconstruction starts*
  - Iterate (P3.1-P3.2), N_3 times.
- Output reconstructed MR image $\boldsymbol{x}$.

GTLMRI: Overall Algorithm

- *Input*: Observation, $\boldsymbol{y} = \mathcal{F}_u \boldsymbol{x}^\star + \eta$; parameters $\lambda, \beta, \tau, \tau', \upsilon, \gamma, \mu$.
- *Goal*: $$\min_{\boldsymbol{W}, \hat{\mathcal{X}}, \mathcal{A}, \boldsymbol{x}} \|\boldsymbol{W}\hat{\mathcal{X}} - \mathcal{A}\|_F^2 + \lambda Q(\boldsymbol{W}) + \beta\|\mathcal{A}\|_1 + \tau\|\mathcal{R}(\boldsymbol{x}) - \hat{\mathcal{X}}\|_F^2 + \eta\|\mathcal{F}_u \boldsymbol{x} - \boldsymbol{y}\|_2^2 + \upsilon'\|\boldsymbol{\Phi x}\|_1$$

- Initialize $\boldsymbol{x} = \mathcal{F}_u^H \boldsymbol{y}$.
- Main iteration:
  - Initialize $\hat{\mathcal{X}} = \mathcal{R}(\boldsymbol{x})$. *denoising starts*
  - Iterate (P2.1), N_1 times.
  - Iterate (P2.2), N_2 times.
  - Initialize $\boldsymbol{x} = \hat{\mathcal{R}}(\hat{\mathcal{X}})$. *reconstruction starts*
  - Iterate (P3.1-P3.2), N_3 times.
- Output reconstructed MR image $\boldsymbol{x}$.

GTLMRI: Overall Algorithm

- *Input*: Observation, $\boldsymbol{y} = \mathcal{F}_u \boldsymbol{x}^\star + \eta$; parameters $\lambda, \beta, \tau, \tau', \upsilon, \gamma, \mu$.
- *Goal*: $$\min_{\boldsymbol{W}, \hat{\mathcal{X}}, \mathcal{A}, \boldsymbol{x}} \|\boldsymbol{W}\hat{\mathcal{X}} - \mathcal{A}\|_F^2 + \lambda Q(\boldsymbol{W}) + \beta \|\mathcal{A}\|_1 + \tau \|\mathcal{R}(\boldsymbol{x}) - \hat{\mathcal{X}}\|_F^2 + \eta \|\mathcal{F}_u \boldsymbol{x} - \boldsymbol{y}\|_2^2 + \upsilon' \|\boldsymbol{\Phi x}\|_1$$

- Initialize $\boldsymbol{x} = \mathcal{F}_u^H \boldsymbol{y}$.
- Main iteration:
  - Initialize $\hat{\mathcal{X}} = \mathcal{R}(\boldsymbol{x})$. *denoising starts*
  - Iterate (P2.1), N_1 times.
  - Iterate (P2.2), N_2 times.
  - Initialize $\boldsymbol{x} = \hat{\mathcal{R}}(\hat{\mathcal{X}})$. *reconstruction starts*
  - Iterate (P3.1-P3.2), N_3 times.
- Output reconstructed MR image $\boldsymbol{x}$.

GTLMRI: Overall Algorithm

- *Input*: Observation, $\boldsymbol{y} = \mathcal{F}_u \boldsymbol{x}^\star + \boldsymbol{\eta}$; parameters $\lambda, \beta, \tau, \tau', \upsilon, \gamma, \mu$.
- *Goal*: $$\min_{\boldsymbol{W}, \hat{\boldsymbol{\mathcal{X}}}, \boldsymbol{\mathcal{A}}, \boldsymbol{x}} \|\boldsymbol{W}\hat{\boldsymbol{\mathcal{X}}} - \boldsymbol{\mathcal{A}}\|_F^2 + \lambda Q(\boldsymbol{W}) + \beta \|\boldsymbol{\mathcal{A}}\|_1 + \tau \|\boldsymbol{\mathcal{R}}(\boldsymbol{x}) - \hat{\boldsymbol{\mathcal{X}}}\|_F^2 + \eta \|\mathcal{F}_u \boldsymbol{x} - \boldsymbol{y}\|_2^2 + \upsilon' \|\boldsymbol{\Phi x}\|_1$$

- Initialize $\boldsymbol{x} = \mathcal{F}_u^H \boldsymbol{y}$.
- Main iteration:
  - Initialize $\hat{\boldsymbol{\mathcal{X}}} = \boldsymbol{\mathcal{R}}(\boldsymbol{x})$. *denoising starts*
  - Iterate (P2.1), N_1 times.
  - Iterate (P2.2), N_2 times.
  - Initialize $\boldsymbol{x} = \hat{\boldsymbol{\mathcal{R}}}(\hat{\boldsymbol{\mathcal{X}}})$. *reconstruction starts*
  - Iterate (P3.1-P3.2), N_3 times.
- Output reconstructed MR image $\boldsymbol{x}$.

Simulations setting

- We compare the reconstruction performance of G-TLMRI algorithm with TLMRI [Ravishankar and Bresler, 2013], DLMRI [Ravishankar and Bresler, 2011] and FCSA [Huang et.al., 2011].
- Simulations for two MR images of size (256×256).
- The downsampling ratio for $\mathcal{F}_u$ is $\kappa/256^2 = 0.25$ (4 fold downsampling) with a random sampling mask.

Simulations setting

- We compare the reconstruction performance of G-TLMRI algorithm with TLMRI [Ravishankar and Bresler, 2013], DLMRI [Ravishankar and Bresler, 2011] and FCSA [Huang et.al., 2011].
- Simulations for two MR images of size (256×256).
- The downsampling ratio for $\mathcal{F}_u$ is $\kappa/256^2 = 0.25$ (4 fold downsampling) with a random sampling mask.

Simulations setting

- We compare the reconstruction performance of G-TLMRI algorithm with TLMRI [Ravishankar and Bresler, 2013], DLMRI [Ravishankar and Bresler, 2011] and FCSA [Huang et.al., 2011].
- Simulations for two MR images of size (256×256).
- The downsampling ratio for $\mathcal{F}_u$ is $\kappa/256^2 = 0.25$ (4 fold downsampling) with a random sampling mask.

Simulations: Original images

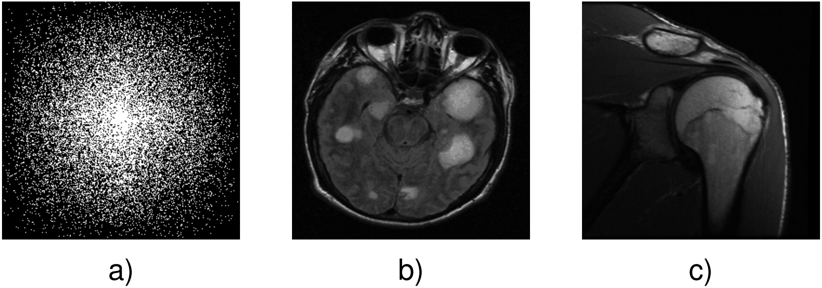

Figure: (a) Sampling mask in k-space with 4-fold undersampling , (b,c) the original MRI test images.

Simulations: Brain image

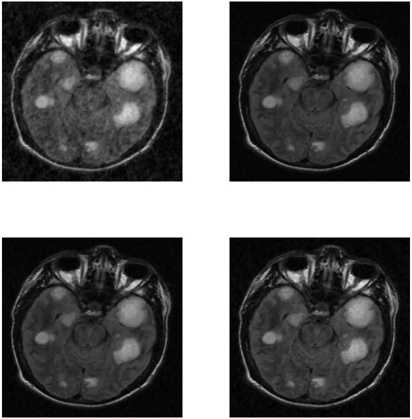

Figure: Brain image results.
First row: Zero-filling and G-TLMRI. Second row: TLMRI and FCSA.

Simulations: Brain image

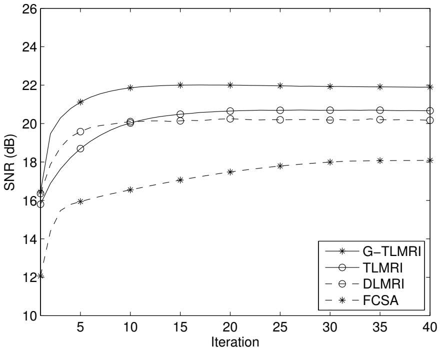

Figure: Brain image results: SNR versus iteration.

Simulations: Shoulder image

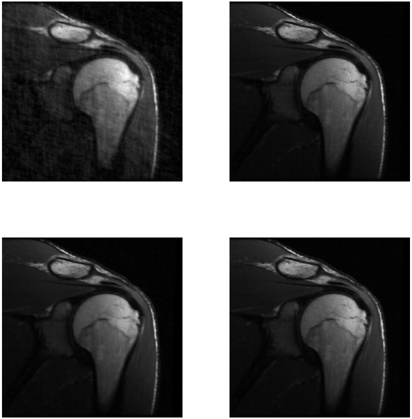

Figure: Shoulder image results.
First row: Zero-filling and G-TLMRI. Second row: TLMRI and FCSA.

Simulations: Shoulder image

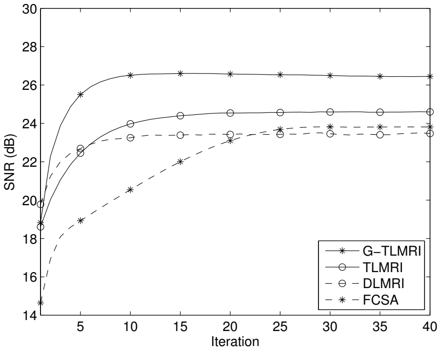

Figure: Shoulder image results: SNR versus iteration.

Conclusion

- We have presented a new algorithm called as G-TLMRI for MRI reconstruction.
- G-TLMRI algorithm builds upon the patch level sparsification of the TLMRI.
- G-TLMRI introduces a global regularizer into the TLMRI framework.
- Combination of the local and global regularization terms results in reconstruction performance exceeding some competing methods which use these terms alone.

Conclusion

- We have presented a new algorithm called as G-TLMRI for MRI reconstruction.
- G-TLMRI algorithm builds upon the patch level sparsification of the TLMRI.
- G-TLMRI introduces a global regularizer into the TLMRI framework.
- Combination of the local and global regularization terms results in reconstruction performance exceeding some competing methods which use these terms alone.

Conclusion

- We have presented a new algorithm called as G-TLMRI for MRI reconstruction.
- G-TLMRI algorithm builds upon the patch level sparsification of the TLMRI.
- G-TLMRI introduces a global regularizer into the TLMRI framework.
- Combination of the local and global regularization terms results in reconstruction performance exceeding some competing methods which use these terms alone.

Conclusion

- We have presented a new algorithm called as G-TLMRI for MRI reconstruction.
- G-TLMRI algorithm builds upon the patch level sparsification of the TLMRI.
- G-TLMRI introduces a global regularizer into the TLMRI framework.
- Combination of the local and global regularization terms results in reconstruction performance exceeding some competing methods which use these terms alone.

- Thanks for listening.

References I

M. Lustig, D. Donoho, and J.M. Pauly,
"Sparse MRI: The application of compressed sensing for rapid MR imaging,"
Magnetic Resonance in Medicine, vol. 58, no. 6, pp. 1182–1195, 2007.

J. Yang, Y. Zhang, and W. Yin,
"A fast alternating direction method for TVL1-L2 signal reconstruction from partial Fourier data,"
IEEE J. Sel. Topics Signal Process., vol. 4, no. 2, pp. 288–297, April 2010.

References II

J.Huang, S.Zhang, and D.Metaxas,
"Efficient MR image reconstruction for compressed MR imaging,"
Medical Image Analysis, vol. 15, no. 5, pp. 670 – 679, 2011.

E.M. Eksioglu,
"Online dictionary learning algorithm with periodic updates and its application to image denoising,"
Expert Systems with Applications, vol. 41, no. 8, pp. 3682 – 3690, 2014.

References III

S. Nam, M.E. Davies, M. Elad, and R. Gribonval,
"The cosparse analysis model and algorithms,"
Applied and Computational Harmonic Analysis, vol. 34, no. 1, pp. 30 – 56, 2013.

S. Ravishankar and Y. Bresler,
"MR image reconstruction from highly undersampled k-space data by dictionary learning,"
IEEE Trans. Med. Imag., vol. 30, no. 5, pp. 1028–1041, May 2011.

References IV

- S. Ravishankar and Y. Bresler,
  "Learning sparsifying transforms,"
  IEEE Trans. Signal Process., vol. 61, no. 5, pp. 1072–1086, 2013.
- E.M. Eksioglu and O. Bayir,
  "K-SVD meets transform learning: Transform K-SVD,"
  IEEE Signal Process. Lett., vol. 21, no. 3, pp. 347–351, March 2014.

References V

S. Ravishankar and Y. Bresler,
"Sparsifying transform learning for compressed sensing MRI,"
in *2013 IEEE 10th International Symposium on Biomedical Imaging (ISBI)*, April 2013, pp. 17–20.

Y. Huang, J. Paisley, Q. Lin, X. Ding, X. Fu, and X.P. Zhang,
"Bayesian nonparametric dictionary learning for compressed sensing MRI,"
IEEE Trans. Image Process., vol. 23, no. 12, pp. 5007–5019, Dec 2014.

References VI

E.M. Eksioglu and O. Bayir,
"Overcomplete sparsifying transform learning algorithm using a constrained least squares approach,"
in *Acoustics, Speech and Signal Processing (ICASSP), 2014 IEEE International Conference on*, May 2014, pp. 7158–7162.

P.L. Combettes and J.C. Pesquet,
"Proximal splitting methods in signal processing,"
in *Fixed-Point Algorithms for Inverse Problems in Science and Engineering*, Optimization and Its Applications, pp. 185–212. Springer New York, 2011.

Sparse MRI

$$\min_{\boldsymbol{x}} \frac{1}{2}\|\mathcal{F}_u\boldsymbol{x} - \boldsymbol{y}\|_2^2 + \rho_1\|\boldsymbol{\Phi}\boldsymbol{x}\|_1 + \rho_2\|\boldsymbol{x}\|_{\mathrm{TV}}.$$

- Several approaches for solving this cost function or its variants.
- In the original Sparse MRI algorithm [Lustig et.al., 2007]: a nonlinear conjugate gradient method
- Operator and variable splitting methods: FCSA, RecPF, TVCMRI ...

Sparse MRI

$$\min_{\boldsymbol{x}} \frac{1}{2}\|\mathcal{F}_u \boldsymbol{x} - \boldsymbol{y}\|_2^2 + \rho_1 \|\boldsymbol{\Phi x}\|_1 + \rho_2 \|\boldsymbol{x}\|_{\mathrm{TV}}.$$

- Several approaches for solving this cost function or its variants.
- In the original Sparse MRI algorithm [Lustig et.al., 2007]: a nonlinear conjugate gradient method
- Operator and variable splitting methods: FCSA, RecPF, TVCMRI ...

Sparse MRI

$$\min_{\boldsymbol{x}} \frac{1}{2}\|\mathcal{F}_u \boldsymbol{x} - \boldsymbol{y}\|_2^2 + \rho_1\|\boldsymbol{\Phi x}\|_1 + \rho_2\|\boldsymbol{x}\|_{\mathrm{TV}}.$$

- Several approaches for solving this cost function or its variants.
- In the original Sparse MRI algorithm [Lustig et.al., 2007]: a nonlinear conjugate gradient method
- Operator and variable splitting methods: FCSA, RecPF, TVCMRI ...